Journal of Medicinal Chemistry

Article

Small Molecule Reversible Inhibitors of Bruton's Tyrosine Kinase (BTK): Structure-Activity Relationships Leading to the Identification of 7-(2-hydroxypropan-2-yl)-4-[2-methyl-3-(4-oxo-3,4-dihydroquinazolin-3-yl)phenyl]-9H-carbazole-1-carboxamide (BMS-935177)

George Vincent De Lucca, Qing Shi, Qingjie Liu, Douglas G. Batt, Myra Beaudoin Bertrand, Richard Rampulla, Arvind Mathur, Lorell N. Discenza, Celia J. D´Arienzo, Jun Dai, Mary T. Obermeier, Rodney Vickery, Yingru Zhang, Zheng Yang, Punit Marathe, Andrew Joseph Tebben, Jodi K. Muckelbauer, ChiehYing J Chang, Huiping Zhang, Kathleen M. Gillooly, Tracy L. Taylor, Mark A. Pattoli, Stacey Skala, Daniel W Kukral, Kim W. McIntyre, Luisa Salter-Cid, Aberra Fura, James R. Burke, Joel C. Barrish, Percy H Carter, and Joseph A Tino

J. Med. Chem., **Just Accepted Manuscript** • DOI: 10.1021/acs.jmedchem.6b00722 • Publication Date (Web): 17 Aug 2016

Just Accepted

ACS Publications

Journal of Medicinal Chemistry is published by the American Chemical Society. 1155 Sixteenth Street N.W., Washington, DC 20036

	Development, Metabolism and Pharmacokinetic Department, Pharmaceutical Candidate Optimization Tebben, Andrew; Bristol-Myers Squibb Pharmaceutical Research and Development, Molecular Structure and Design, Molecular Discovery Technologies Muckelbauer, Jodi; Bristol-Myers Squibb Pharmaceutical Research and Development, Molecular Structure and Design, Molecular Discovery Technologies Chang, ChiehYing; Bristol-Myers Squibb Pharmaceutical Research and Development, Molecular Structure and Design, Molecular Discovery Technologies Zhang, Huiping; Bristol-Myers Squibb Pharmaceutical Research and Development, Discovery Chemistry Gillooly, Kathleen; Bristol-Myers Squibb, Immunology biology Taylor, Tracy; Bristol-Myers Squibb Pharmaceutical Research and Development, Discovery Biology Pattoli, Mark; Bristol-Myers Squibb Pharmaceutical Research and Development, Discovery Biology Skala, Stacey; Bristol-Myers Squibb Pharmaceutical Research and Development, Discovery Biology Kukral, Daniel; Bristol-Myers Squibb Pharmaceutical Research and Development, ECTR/CTTO Imaging Department McIntyre, Kim; Bristol-Myers Squibb Pharmaceutical Research and Development, Discovery Biology Salter-Cid, Luisa; Bristol-Myers Squibb Pharmaceutical Research and Development, Discovery Biology Fura, Aberra; Bristol-Myers Squibb Pharmaceutical Research and Development, Metabolism and Pharmacokinetic Department, Pharmaceutical Candidate Optimization Burke, James; Bristol-Myers Squibb Pharmaceutical Research and Development, Discovery Biology Barrish, Joel; Bristol-Myers Squibb Pharmaceutical Research and Development , Discovery Chemistry Carter, Percy; Bristol-Myers Squibb Pharmaceutical Research and Development, Discovery Chemistry Tino, Joseph; Bristol-Myers Squibb Pharmaceutical Research and Development, Discovery Chemistry

Small Molecule Reversible Inhibitors of Bruton's Tyrosine Kinase (BTK): Structure-Activity Relationships Leading to the Identification of 7-(2-hydroxypropan-2-yl)-4-[2-methyl-3-(4-oxo-3,4-dihydroquinazolin-3-yl)phenyl]-9H-carbazole-1-carboxamide (BMS-935177)

George V. De Lucca,[a] Qing Shi,[a] Qingjie Liu,[a] Douglas G. Batt,[a] Myra Beaudoin Bertrand,[a] Rick Rampulla,[a] Arvind Mathur,[a] Lorell Discenza,[d] Celia D'Arienzo,[d] Jun Dai,[d] Mary Obermeier,[d] Rodney Vickery,[d] Yingru Zhang,[d] Zheng Yang,[d] Punit Marathe,[d] Andrew J. Tebben,[c] Jodi K. Muckelbauer,[c] ChiehYing J. Chang,[c] Huiping Zhang,[a] Kathleen Gillooly,[b] Tracy Taylor,[b] Mark A. Pattoli,[b] Stacey Skala,[b] Daniel W. Kukral,[e] Kim W. McIntyre,[b] Luisa Salter-Cid,[b] Aberra Fura,[d] James R. Burke,[b] Joel C. Barrish,[a] Percy H. Carter,[a] and Joseph A. Tino*[a]*

[a]Immunosciences Discovery Chemistry, [b]Immunoscience Discovery Biology, [c]Molecular Structure and Design, Molecular Discovery Technologies, [d]Metabolism and Pharmacokinetic Department, Pharmaceutical Candidate Optimization, and [e]ECTR/CTTO Imaging Department, Bristol-Myers Squibb Research and Development, P.O. Box 4000, Princeton, New Jersey 08543

RECEIVED DATE

ABSTRACT: Bruton's Tyrosine Kinase (BTK) belongs to the TEC family of non-receptor tyrosine kinases, and plays a critical role in multiple cell types responsible for numerous autoimmune diseases. This article will detail the structure-activity relationships (SAR) leading to a novel second generation series of potent and selective reversible carbazole inhibitors of BTK. With an excellent pharmacokinetic profile as well as demonstrated *in vivo* activity and an acceptable safety profile, 7-(2-hydroxypropan-2-yl)-4-[2-methyl-3-(4-oxo-3,4-dihydroquinazolin-3-yl)phenyl]-9H-carbazole-1-carboxamide **6** (**BMS-935177**) was selected to advance into clinical development.

INTRODUCTION

Kinases continue to be a very active area for drug discovery, targeting treatments in a wide range of therapeutic areas.[1] Bruton's Tyrosine Kinase (BTK) is a non-receptor tyrosine kinase expressed in all hematopoietic cells except plasma and T cells. Although only one of the five mammalian TEC family members, BTK is the most important from a target perspective since it is critical for B cell signaling through the B cell receptor (BCR).[2] In addition to B cells, BTK is vital for signaling in low affinity activating Fcγ receptors (e.g., FcγRIII and FcγRIIa) in monocytic cells. BTK also regulates the expression of proinflammatory cytokines, chemokines and cell adhesion molecules in response to receptor activation through FcεRI signaling in mast cells and basophils.[3] RANK signaling, which controls osteoclastogenesis from monocytic precursors, is also BTK-dependent.[4]

B cells are essential to the pathogenesis of autoimmune diseases such as rheumatoid arthritis (RA) as demonstrated by the clinical results for the B cell-depleting anti-CD20 antibody rituximab.[5] In addition to producing autoantibodies, B cells can control autoimmunity as sources of proinflammatory chemokines and cytokines, such as IL-6 and TNFα, and through their role as antigen-presenting cells.[6] Because BTK kinase activity is necessary for BCR-dependent proliferation of B cells as well as production of proinflammatory cytokines and costimulatory molecules (e.g., CD86), pharmacological inhibition of BTK is expected to affect several pathways by which B cells may mediate autoimmunity, but without depleting B cells. Pharmacological and genetic studies in animal models strengthen the case that BTK inhibitors would be efficacious against autoimmune indications such as RA or systemic lupus erythematosus (SLE). BTK-deficient mice are less sensitive to both the (NZB X NZW)F1 model of lupus and the collagen-induced arthritis (CIA) model.[7] BTK inhibitors reduce disease progression in the collagen antibody-induced arthritis (CAIA) and CIA models, in addition to murine lupus models.[8] The vital role of BTK in B cells is also observed in human x-linked agammaglobulinemia (XLA)

immunodeficiency. XLA patients have inactivating mutations in the BTK gene leading to a loss of mature B cells and circulating antibodies.[9]

A key structural feature of the BTK kinase domain is the non-catalytic cysteine (Cys481) residue in the extended hinge region.[10] Numerous companies have targeted this residue to prepare irreversible BTK inhibitors, with the most successful being ibrutinib (**1**; Pharmacyclics/J&J), which is approved for various non-Hodgkin's lymphomas (Figure 1).[11,12] Several additional BTK inhibitors have entered clinical trials for the treatment of autoimmune indications, including covalent inhibitors from Celgene (**2**), Hanmi (**3**) and Principia (**4**, structure unknown, 2014 press release),[13] with the most advanced appearing to be **2**, currently in Phase II trials in RA (Figure 1).[14] Efficacy results for these and other compounds entering clinical trials are eagerly awaited, since small molecule inhibitors of this mechanism have the potential to compete with biologics for the treatment of RA and several other autoimmune diseases. In addition to these covalent inhibitors, recent reports from Roche and Merck show continued interest in reversible BTK inhibitors.[15,16]

We have previously disclosed the discovery of a novel carbazole series of BTK inhibitors, as well as the initial structure-activity relationships (SAR) leading to **5** (Figure 2).[17] Compound **5** inhibited BTK with modest kinase selectivity. Having identified a novel carbazole series of BTK inhibitors, we began an effort to address the liabilities of **5** and similar analogs. In the current paper, we disclose carbazoles with improved oral exposure, kinase selectivity and BTK potency, leading to the discovery of the clinical development candidate **6** (BMS-935177)[17b].

RESULTS AND DISCUSSION

As we have reported previously, X-ray structural data for a member of the carbazole carboxamide series showed that the carbazole NH and both the carbonyl and NHs of the primary amide formed critical hydrogen bonds to the key hinge region of BTK.[17a] It was also noted that a small ortho-substituent on the C-4 phenyl ring improved both BTK potency and kinase selectivity when compared

to the parent unsubstituted analog. In addition, X-ray structures showed the C-7 substituent bound in the solvent exposed extended hinge region of BTK.[17a] Several initial issues for the carbazole series required optimization, including kinase potency and selectivity, as well as oral exposure in mouse. Our efforts to address these concerns involved the use of a combination of focused library and individual analog synthesis as outlined in Figure 3. The 4-fluorophenyl amide of **5** was replaced with a variety of alkyl, aryl, and heteroaryl amides as well as ureas and carbamates using the aniline **7a**. To explore the SAR at the C-7 position, the piperazine of amide of **5** was replaced with a variety of alkyl, aryl, and heteroaryl amides starting from the acid **8a**. The acid substituent of a **8a** precursor was converted to aniline **9a** (see experimental section) which was used as the starting material to further explore the SAR at C-7 to give **9b**, incorporating a variety of alkyl anilines as well as a range of alkyl, aryl, and heteroaryl amides, ureas and carbamates. From this thorough exercise two analogs were noteworthy, **10** and **11** (Table 1).

The polarity of the piperazine amide C-7 substituent coupled with the large number of hydrogen bond donors and acceptors in **5** led to low permeability as measured in PAMPA, contributing to low oral exposure in mouse (Table 1). The ortho–pyridyl analog **10**, designed to form an intra-molecular H-bond with the amide NH to improve permeability, maintained good BTK potency with improved PAMPA and oral exposure as shown in Table 1, although selectivity over the SRC family of kinases (LCK as an example found on T-cells) was still unacceptable. The goal of >50-fold selectivity over the SRC family was set to minimize the chances of being too immunosuppressive in vivo by targeting both B- and T-cells. Recognizing that the C-7 substituents could potentially bind in the solvent exposed extended hinge region of BTK, modification of the side chain could be used to "tune" the properties of inhibitors. Analog exploration at C-7 (Figure 3) often showed a dramatic effect on kinase selectivity and potency. However, many of these analogs were of high molecular weight with low oral plasma concentrations in mouse PK studies (results not shown). The amino acid at the C-terminal end of the hinge in BTK, Ala478, is often an acidic residue in SRC kinase family members such as LCK (Glu 320). We predicted that a less basic C-7 group could improve selectivity over the piperazine amide. In order to keep the

molecular weight low, compound **11** was prepared and found to be a potent BTK inhibitor with improved oral plasma exposure and LCK kinase selectivity (Table 1). However, analogs with a pendant meta-aryl or heteroaryl amide substituent on the C-4 phenyl, as in **10** and **11**, showed hydrolysis to an aniline metabolite as the major metabolic pathway in human and rat liver microsomes. In addition, in the case of **11**, concomitant N-dealkylation of the iso-propyl group led to the corresponding bis-aniline metabolite, observed in both liver microsomes and as a circulating metabolite after oral dosing in mice. Upon multiple day dosing in mice, compound **11** showed toxicity in vivo that could be attributed to the bis-aniline metabolite (data not shown). Predicting the extent of amide hydrolysis in humans based on pre-clinical data is potentially challenging,[18] supporting the decision to stop further progression of these analogs.

To avoid any possible aniline release, numerous medicinal chemistry approaches to stabilize amide hydrolysis were investigated. The most direct approach, synthesis of the cyclic amides, was also the most effective. The five-membered ring lactam **12** maintained BTK potency with acceptable permeability (PAMPA Pc 494 nm/s, Table 2). As expected, **12** was stable to hydrolysis in vivo, however the plasma concentration in mouse was similar to **5**, which also contained the piperazine amide. It should be noted that the mouse liver microsome metabolic stability[25e] of the three compound **5**, **10**, and **12** containing the piperazine amide were comparable. It was surprising that the exposure for lactam **12** was significantly worse than that of ortho–pyridyl analog **10**, designed to form an intra-molecular H-bond with the amide NH, which points to the difficulty of predicting exposure based solely on one parameter, such as numbers of hydrogen bonds.

The SAR results from our previous C-7 analogs prepared for compound **5** (outlined in Figure 3), suggested that small polar non-basic or weakly basic groups would be best for potency, selectivity, and PAMPA. Combining the C-4 lactam with a tertiary carbinol as a C-7 substituent led to analog **13** which maintained BTK potency and improved potency in the Ramos B cell calcium flux assay (Table 2). In order to further optimize **13**, a second survey of alternate C-7 substituents was undertaken focusing on

small polar groups. Ultimately, no other substituent was found to give better overall properties than the carbinol. An investigation of substituents on the phenyl ring of the lactam identified the fluoro-substituted analog **14**, which had improved BTK cell potency and mouse liver microsome metabolic stability compared to **13**. Compound **14** showed significantly improved oral plasma concentrations in mouse compared to **12** (Table 2), suggesting that it was suitable for further in vivo studies.

BTK regulates antigen receptor (BCR) signaling in B cells, and one of the hallmarks of xid (x-linked immune defect) mice deficient in BTK is a defective neoantigen-induced antibody response. As a result, it was anticipated that activity against a keyhole limpet hemocyanin (KLH) induced antibody response in mice would provide an important pharmacodynamics (PD) readout of BTK inhibition.[19] In this model, anti-KLH antibodies of the IgM isotype appear in the first week after challenge, followed by isotype switching to IgG anti-KLH antibodies evident by day 14. However, **14** showed only a non-statistically significant decrease in IgG when dosed orally at 30 mg/kg BID in the chronic KLH mouse model. The weak suppression of the anti-KLH response, coupled with a non-optimal PK profile, prohibited further advancement of compound **14**.

An extensive exploration of heterocyclic analogs of **14** was conducted to find compounds with improved potency and oral plasma concentrations (Table 2). BTK potency was maintained in several 6, 6 bicyclic ring systems, such as in analogs **15** and **16**, but they were either less LCK (or other kinase) selective or less potent in cells than **14**. The unsubstituted quinazolinone **6** showed improved Ramos B cell potency with similar LCK selectivity to **14**. Quinazolinones were substituted with an array of electron donating and withdrawing groups, as well as a range of both polar and lipophilic moieties. However, in none of these cases was the overall profile improved over the unsubstituted parent analog **6**. For example, a fluoro scan on the quinazolinone ring provided **17**-**20**. Although all of the fluoro analogs were potent BTK inhibitors, none showed significant improvements over **6**. All five analogs were investigated in mouse PK studies at 10 mpk, showing improved oral plasma concentrations compared to **14** (Table 2). Quinazolinone analogs **21** (Table 2) and **22** (Table 3) were also prepared to

investigate the requirements of the tertiary carbinol and the ortho-methyl substituent in the C-4 aryl linker, respectively. Compound **21** maintained BTK enzyme potency, but showed lower oral plasma concentrations in mouse compared to **6**. Analog **22** had a significant drop in BTK enzyme potency, highlighting the importance of the C-4 aryl ortho-methyl substituent.

Attempts to obtain an X-ray co-crystal structure of **6** bound to BTK were unsuccessful. However, close analog **23** (Table 3) provided a 1.9 Å X-ray crystal structure bound to the active site of BTK (PDB ID 5JRS. Authors will release the atomic coordinates and experimental data upon article publication.), as shown in Figure 4. The carbazole NH and primary amide were bound to the hinge as expected,[17a] forming crucial hydrogen bonds with the backbone carbonyl of Met-477 and both the backbone NH of Met-477 and the carbonyl of Glu-475, respectively. In addition, the primary amide formed a third hydrogen bond to a water in the gate keeper region, which was linked to an extensive water network that filled the pocket. The fluorophenyl ring was nearly orthogonal to the carbazole, with the ortho fluoro filling a small hydrophobic pocket formed by Leu-528 at the base of the ATP pocket and the backbone of Cys-481. The quinazolinone ring was in turn orthogonal to the C-4 phenyl linker, with the carbonyl interacting with a conserved water in the extended hinge region. Finally, the C-7 tertiary carbinol was water-exposed in the extended hinge region as predicted, stabilizing a water network that also included the quinazolinone carbonyl.

Although several analogs displayed in Table 2 showed promising plasma concentrations in mouse, none displayed a superior profile for progression compared to the parent quinazolinone **6**. With the low aqueous solubility (<1 μg/mL) of **6**, further lipophilic fluoro substituents in **17-20** could be problematic in achieving dose linear oral exposures in further animal studies. Therefore, compound **6** was selected for detailed in vitro and in vivo characterization.

A partial list of kinase selectivity data for compound **6** is summarized in Table 4. Compound **6** is a potent, reversible inhibitor of BTK (IC_{50} 2.8 nM) and demonstrated good kinase selectivity when tested against a screening panel of 384 kinases at DiscoveRx (Fremont, CA; formally Ambit Biosciences),[20]

with only 16 kinases showing less than 15% control binding at 1000 nM. Consistent with this measure of selectivity, biochemical kinase assays against 60 kinases showed **6** to be more potent against BTK than any other kinase, including the other Tec family kinases (TEC, BMX, ITK and TXK) over which the compound is between 5- and 67-fold selective. With the exception of 7-fold selectivity over BLK, expressed specifically in B cells, the compound showed greater than 50-fold selectivity over the SRC family of kinases, including 1,100-fold selectivity over SRC itself. Other kinases inhibited with a potency less than 150 nM (50-fold selectivity) included TRKA, HER4, TRKB, and RET.

Cell potency data for compound **6** is summarized in Table 5. In B cells stimulated through the BCR, **6** selectively inhibited several different readouts. Compound **6** inhibited calcium flux in human Ramos B cells (IC_{50} 27 nM) and inhibited CD69 surface expression in peripheral B cells stimulated with anti-IgM and anti-IgG. However, **6** had no effect on CD69 surface expression in B cells stimulated through the CD40 receptor with CD40 ligand. Against IgG-containing immune complex-driven low affinity activating Fcγ receptor (FcγRIIa and FcγRIII) endpoints in peripheral blood mononuclear cells (PBMCs), **6** effectively inhibited TNFα production with an IC_{50} value of 14 nM. To determine the whole blood potency, the ability of the compound to inhibit BCR-stimulated expression of CD69 on the surface of B cells in whole blood was measured in a FACS-based assay which allowed for gating on the B cells. Against this BTK-dependent endpoint, **6** showed mean IC_{50} values of 550 ± 100 (n=11) and 2060 ± 240 nM (n=3) in human and mouse whole blood, respectively. The somewhat more potent inhibition in human compared to mouse whole blood may reflect both an intrinsic human potency advantage, as well as protein binding differences between species (Table 6).

Some of the detailed in vitro profiling data for compound **6** is summarized in Table 6. Plasma protein binding for **6** was high for all species, with less than 1% free for human. The high protein binding could mitigate the effects of the hERG patch clamp IC_{50} of ~10 μM. Although the crystalline aqueous solubility was <1 μg/mL for **6**, simulated gastric fluid showed improved solubility, both in fed and fasted state solutions. The high PAMPA permeability and low aqueous solubility placed **6** in the

BCS Class 2 category. The Caco-2 values showed that **6** is a PgP substrate, although this is mitigated by the high passive permeability.

In the KLH assay, **6** showed superior in vivo potency compared to **14**. As shown in Figure 5a, when dosed orally once daily at 5, 20 and 45 mg/kg to mice the compound inhibited anti-KLH antibodies of the IgG isotype at day 14, with statistically significant reductions at all doses. In satellite mice from this study dosed with **6** at 5 mg/kg, the plasma concentration was maintained above the mouse whole blood BCR-stimulated CD69 IC_{50} value of 2 μM for only approximately five hours (see Figure 5b). However, this transient daily coverage at the low dose yielded a significant inhibition of IgG anti-KLH titers, indicating that significant pharmacological activity can be observed even with incomplete coverage of the whole blood IC_{50} potency.

Figure 6 shows the results of fully preventative dosing with **6** in a mouse CIA model. At once daily oral doses of 10, 20 and 30 mg/kg beginning on the day of primary immunization, **6** provided a clear dose-dependent reduction in both the severity and incidence of clinically evident disease in this rodent model of RA. At 10 mg/kg of **6**, disease severity was reduced about 40% compared to vehicle treatment, and the percentage of animals showing any signs of disease was reduced by a third. At the 10 mg/kg dose the plasma level of **6** was maintained above the mouse WB IC_{50} of 2.06 μM (Table 5) for 12 hours, with a 24 hour trough level of 277 nM. At the two higher doses of 20 and 30 mg/kg, disease severity was reduced by 85-90% compared to vehicle treatment, and disease incidence was reduced by two-thirds. At the 20 mg/kg dose the plasma level of **6** was maintained above the mouse WB IC_{50} for 20 hours, with a 24 hour trough plasma level of 1171 nM. At the end of the study, the tibiotarsal joints were evaluated histologically and graded semi-quantitatively for severity of inflammation, synovial hyperplasia, bone resorption, and cartilage erosion. Consistent with the clinically observed effects on disease incidence and severity, **6** dose-dependently inhibited both inflammation and bone resorption endpoints (Figure 7). Micro-computed tomography of the hind limbs also showed that **6** provided a dose-dependent protection against the pitting, loss of bone mass, woven porous bone, and fusion of the

small bones evident in the mice receiving only vehicle, with the animals receiving 20 mg/kg showing essentially complete protection as evidenced by the presence of a smooth bone surface and easily recognizable small individual bones of the foot and ankle (representative images in Figure 8). The compound was also effective at 30 mg/kg PO QD in blocking disease progression when administration of **6** is initiated after the booster immunization (pseudo-established dosing mode; data not shown).

In the B cell independent mouse CAIA disease model, **6** was also efficacious, reflecting the involvement of activating Fcγ receptor pathways which were blocked by BTK inhibition.[21] Figure 9 shows that QD oral doses of 10 and 30 mg/kg provided a significant, dose-dependent reduction in paw clinical scores. Indeed, mice receiving **6** at 30 mg/kg were virtually disease-free throughout the period of the study, and this regimen was more effective in this model than dexamethasone. These results indicate that inhibition of BTK by **6** in signal transduction pathways and cells (e.g., activating Fcγ receptors in monocytic cells) other than BCR signaling is likely contributing to the profound efficacy seen in the CAIA and CIA models of arthritis.

One of the strongest attributes of compound **6** is excellent oral bioavailability in all pre-clinical species, both from suspension and solution dosing, despite its low aqueous solubility. The oral bioavailability for **6** with solution dosing ranges from 84 to 100% in rat, mouse, dog and cynomolgus monkey, with low clearance in single intravenous (IV) infusion studies (summarized in Table 7). When dosed as a crystalline micro-suspension in rats (5 mpk in citrate buffer at pH 4, with 0.02% DOSS and 0.5% methocel) **6** maintained excellent oral bioavailability of ~100%. Projections based on the good pharmacokinetics across species as well as efficacy in mouse models suggested that compound **6** could provide significant clinical benefit with once a day dosing.

Chemistry

The general synthetic route utilized in the preparation of the bicyclic amide replacement carbazole analogs in Tables 2 and 3 is outlined in Scheme 1. The key reaction was a Suzuki coupling between the appropriate partners **24** and **25**. Bromo carbazoles **24** (**Y^1=Br**) were reacted with boronic esters **25**

(Z^1=boronic ester) under Suzuki coupling conditions to give final compounds **6** and **12-23**.[22,23] Alternatively, the partners could be reversed with the carbazole boronic esters **24** (**Y^1= boronic ester**) reacting with the bromide **25** (**Z^1=Br**) using the same coupling condition to give the final products in generally good yields. The C-7 functionalized carbazole intermediates were prepared as shown in Schemes 2-3. The Fischer indole cyclization using ketone **26** and hydrazine **27** was accomplished by heating in acetic acid to give the tetrayhdrocarbazole **28** in 58% yield. Acid intermediate **28** was activated with EDC and HOBt, then treated with ammonium hydroxide to give amide **29** in 76% yield. Aromatization of **29** with DDQ gave ester carbazole **30** in good yield. Reduction of **30** with lithium aluminum hydride gave the benzyl alcohol intermediate **32** (64% yield). The tertiary carbinol intermediate **31** was prepared directly from ester **30** using methyl lithium in 84% yield. Ester **30** was hydrolyzed with LiOH to acid **34** which was then coupled with *N*-methyl piperazine in the presence of EDC and HOBt to provide bromo amide **35** in excellent yield (Scheme 3). Alternatively, acid **34** was subjected to a Curtius rearrangement to give the Cbz-protected intermediate **36**, allowing access to C-7 amino analogs **9a** and **9b** shown in Figure 3.

The bromo amide intermediate **35** underwent a Suzuki reaction with 2-methyl-3-(4,4,5,5-tetramethyl-1,3,2-dioxaboralan-2-yl)aniline to give intermediate **7a** in 77% yield as shown in Scheme 4. Coupling of **7a** with the appropriate acid then provided the final amides **5** or **10** in good yields. Alternatively, the bromo intermediate **35** was subjected to a Suzuki reaction with boronic ester **40a** to give the lactam **12** in 60% yield (Scheme 4). The synthesis of **40a** is summarized in Scheme 5. The bromo aniline **37** was acylated with 2-(chloromethyl)benzoyl chloride **38** and the resulting amide intermediate was cyclized in the presence of a base to give the bromo lactam **39a**. Treatment with bis(pinacolato)diboron under standard conditions gave high yields of the boronic ester **40a**.

The other key Suzuki partners required for the preparation of final compounds **6** and **13-23** were synthesized as shown in Schemes 6-7. The preparations of isoquinolinone **44** and 3,4-dihydroisoquinolinone **47** are summarized in Scheme 6. The condensation of bromo aniline **41** with cyclic anhydride **42** provided the corresponding cyclic imide which was subsequently reduced with

$NaBH_4$ and dehydrated under acidic conditions to give bromo-isoquinolinone **43**. The bromo isoquinolinone was then converted to the boronic ester **44** in good yield. The reaction of 1,3-dibromo-2-methylbenzene **45** with 3,4-dihydroisoquinolin-1(2H)-one **46** in the presence of CuI gave the bromo dihydroisoquinolin-1(2H)-one **47** used to synthesize final compound **15**. The quinazolinones were obtained by the reaction of bromo anilines **48** with anthranilic acids **49** in the presence of triethyl orthoformate to give the bromo quinazolinones **50** in moderate to good yields (Scheme 7). The bromo quinazolinones were then converted to the required boronic esters **51** in good yields. With the appropriate Suzuki partners prepared, the assembly of the final compounds (**6** and **12-23**, Tables 2-3) was carried out under standard cross-coupling conditions in good yields as summarized in Scheme 1.

During the analysis of the NMR data of final analogs such as **6**, complex splitting patterns were observed. Hindered rotation of the carbazole C-4 bond as well as the bond to the quinazolinone caused by the ortho-methyl substituent on the phenyl linker (Figure 10) created atropisomers. Chiral SFC chromatography was able to separate the four possible atropisomers, although they could not be isolated without racemization back to the original mixture due to the low barrier to rotation at room temperature.

Conclusion

In summary, a novel second generation series of carbazole BTK inhibitors has been identified. The potential problem of aniline formation from benzamides such as **5**, **10** and **11** was solved by conversion to the corresponding lactams (such as **12**). Oral exposure was improved by replacing the C-7 substituent with the less-polar tertiary carbinol. Extensive exploration of other heteroaryl modifications of the lactam moiety provided 7-(2-hydroxypropan-2-yl)-4-[2-methyl-3-(4-oxo-3,4-dihydroquinazolin-3-yl)phenyl]-9H-carbazole-1-carboxamide **6**, a potent BTK inhibitor with improved kinase selectivity and superior oral exposure in multiple species. These features, coupled with robust efficacy in mouse arthritis models dependent on both B cell and non-B cell mechanisms, predict that **6** should provide useful clinical efficacy in autoimmune diseases. Based on in vitro potency, in vivo activity and

pharmacokinetic profile, compound **6** was selected for further studies in support of clinical development.

Experimental Section

General Procedures. All reagents were purchased from commercial sources and used without further purification unless otherwise noted. All reactions were performed under an inert atmosphere of nitrogen or argon. Chromatographic purification was conducted on pre-packed silica gel cartridges using a flash chromatography system such as the CombiFlash®Rf+System (Teledyne ISCO). HPLC and LCMS analyses were conducted using a Shimadzu SCL-10A liquid chromatograph and a SPD UV-Vis detector at 220 or 254 nm with the MS detection performed with either a Waters Micromass ZQ spectrometer or a Micromass Platform LC spectrometer. Unless otherwise reported, preparative reverse-phase HPLC purifications were performed using the following conditions: YMC S5 ODS 20 x 100 mm column with a binary solvent system where solvent A = 10% methanol, 90% water, 0.1% trifluoroacetic acid and solvent B = 90% methanol, 10% water, and 0.1% trifluoroacetic acid, flow rate = 20 mL/min, linear gradient time = 10 min, start %B = 20, final %B = 100. Fractions containing the product were concentrated in vacuo to remove solvent. The resulting product could be further neutralized with aqueous sodium bicarbonate, extracted into organic solvent, dried and concentrated under reduced pressure. Proton nuclear magnetic resonance (^{1}H NMR) spectra were recorded on either a JEOL Eclipse 500 or a Bruker Avance 400 spectrometer and are reported in ppm relative to either residual protio-solvent of the sample in which they were run or to TMS as internal standard. Coupling constants are provided in Hz with standard abbreviations for the spectral pattern designations.

HPLC analyses for purity were performed using the following two conditions for all final compounds and were determined to have an HPLC purity of $\geq 95\%$ unless otherwise noted.

Method A: A linear gradient using 5% acetonitrile, 95% water, and 0.05% TFA (Solvent A) and 95% acetonitrile, 5% water, and 0.05% TFA (Solvent B); t = 0 min., 10% B, t = 12 min., 100% B (15 min.)

was employed on a Waters SunFire C_{18} 3.5µ 4.6 x 150 mm column. Flow rate was 1.0 ml/min and UV detection was set to 220/254 nm. The column was maintained at ambient temperature.

Method B: A linear gradient using 5% acetonitrile, 95% water, and 0.05% TFA (Solvent A) and 95% acetonitrile, 5% water, and 0.05% TFA (Solvent B); *t* = 0 min., 10% B, *t* = 12 min., 100% B (15 min.) was employed on a Waters XBridge Ph 3.5µ 4.6 x 150 mm column. Flow rate was 1.0 ml/min and UV detection was set to 220/254 nm. The column was maintained at ambient temperature.

4-(3-(4-Fluorobenzamido)-2-methylphenyl)-7-(4-methylpiperazine-1-carbonyl)-9H-carbazole-1-carboxamide, TFA (5).

Step A. Ethyl 3-hydroxycyclohexanecarboxylate. To an EtOH (500 mL) solution of ethyl 3-hydroxybenzoate (50 g, 0.3 mol) was added 5% rhodium on alumina (7.5 g) and the mixture was stirred in an autoclave under 12 kg hydrogen pressure at RT overnight. The reaction mixture was filtered through Celite and the volatiles removed to give ethyl 3-hydroxycyclohexanecarboxylate (50 g, 96%) as a liquid and a mixture of diastereomers. The material was used without further purification. Mass spectrum *m/z* 173 $(M+H)^+$. ^{1}H NMR ($CDCl_3$, 400 MHz) δ 4.03-4.21 (m, 2.3H), 3.54-3.71 (m, 0.7H), 2.67-2.83 (m, 0.3H), 2.36 (m, 0.7H), 2.20 (m, 1H), 1.76-2.01 (m, 3H), 1.16-1.76 (m, 8H).

Step B. Ethyl 3-oxocyclohexanecarboxylate (26). To a DCM (1.1 L, dry) solution of ethyl 3-hydroxycyclohexanecarboxylate (51 g, 0.3 mol) at 0 ^{o}C was added carefully portion-wise Dess-Martin periodinane (251 g, 0.59 mol). After the addition was complete, the reaction mixture was allowed to slowly come to RT overnight. The reaction was basified by the addition of Na_2CO_3 solution, the resulting solids removed by filtration through Celite, and the filtrate concentrated. The resulting residue was diluted with EtOAc, the organic layer washed with Na_2CO_3 solution, water, brine, dried over Na_2SO_4 and concentrated to give **26** (48 g, 95%) as a lightly yellow colored oil. The ester **26** had a very strong odor and should be handled in a fume hood. Mass spectrum *m/z* 171 $(M+H)^+$. ^{1}H NMR (400 MHz, $CDCl_3$) δ 4.16 (q, *J*=7.1 Hz, 2H), 2.78 (s, 1H), 2.55 (d, *J*=8.3 Hz, 2H), 2.28-2.43 (m, 2H), 2.03-2.16 (m, 2H), 1.68-1.90 (m, 2H), 1.27 (t, *J*=7.0 Hz, 3H).

Step C. 4-Bromo-2-hydrazinylbenzoic acid (27). A solution of sodium nitrite (2.4 g, 35.5 mmol) in water (12 mL) was added drop-wise to a suspension of 2-amino-4-bromobenzoic acid (7.3 g, 33.8 mmol) in concentrated aqueous hydrochloric acid (34 mL) at -5 °C, at such rate that the temperature did not exceed 0 °C. The resulting suspension was stirred at -5 °C for 10 min and was then added drop-wise to a rapidly stirred solution of tin (II) chloride (13.5 g, 71.0 mmol) in concentrated aqueous hydrochloric acid (10 mL) at -5 °C at such a rate that the temperature did not exceed 0 °C. The resulting suspension was warmed to RT and stirred for 1h. The precipitate was collected by filtration, washed with water, and air-dried to afford **27** (7.8 g, 86%) as a light-colored solid. Mass spectrum *m/z* 231.0, 233.0 $(M+H)^+$.

Step D. 5-Bromo-2-(ethoxycarbonyl)-2,3,4,9-tetrahydro-1*H*-carbazole-8-carboxylic acid (28). A stirred suspension of **27** (16.4 g, 58.1 mmol) in acetic acid (171 mL) was treated with **26** (9.9 g, 58.1 mmol) at RT. The mixture was stirred at reflux for 2.5 h. The mixture was cooled to RT and concentrated to afford a brown solid. The solid was suspended in ethyl acetate (20 mL) and the precipitate was collected by filtration, washed with ethyl acetate and air dried to provide **28** (11.5 g) as a colorless solid. The filtrate was concentrated, the residue resuspended in ethyl acetate, and the precipitate collected by filtration to provide additional **28** (0.8 g, total 12.3 g, 58%). Mass spectrum *m/z* 366.0, 368.0 $(M+H)^+$. ^{1}H NMR (400 MHz, DMSO-d_6) δ 13.10 (br s, 1H), 11.06 (s, 1H), 7.50 (d, *J*=8.13 Hz, 1H), 7.19 (d, *J*=8.13 Hz, 1H), 4.07-4.15 (m, 2H), 3.08-3.19 (m, 1H), 2.99-3.08 (m, 1H), 2.89-2.99 (m, 2H), 2.79-2.89 (m, 1H), 2.09-2.22 (m, 1H), 1.75-1.89 (m, 1H), 1.20 (t, *J*=7.14 Hz, 3H).

Step E. Ethyl 5-bromo-8-carbamoyl-2,3,4,9-tetrahydro-1*H*-carbazole-2-carboxylate (29). A suspension of acid **28** (12.3 g, 33.5 mmol), EDC (7.7 g, 40.2 mmol), and 1-hydroxybenzotriazole hydrate (6.2 g, 40.2 mmol) in THF-DCM (4:1, 335 mL) was treated with aqueous ammonium hydroxide (7.83 mL, 201 mmol), and the resulting suspension was stirred at RT overnight. The mixture was concentrated and the residue was suspended in water. The precipitate was collected by filtration, washed with water and ethyl acetate and air dried to give **29** (8.9 g). The filtrate was concentrated and the residue was suspended in methanol. A solid was collected by filtration, washed with methanol and air dried to afford additional **29** (0.4 g, total 9.3 g, 76%). Mass spectrum *m/z* 365.1, 367.1 $(M+H)^+$. ^{1}H

NMR (400 MHz, DMSO-d_6) δ 11.08 (s, 1H) 8.02 (br s, 1H), 7.43 (d, *J*=8.13 Hz, 1H), 7.39 (br s, 1H), 7.14 (d, *J*=8.13 Hz, 1H), 4.02-4.17 (m, 2H), 3.07-3.18 (m, 1H), 2.97-3.06 (m, 1H), 2.86-2.98 (m, 2H), 2.77-2.86 (m, 1H), 2.09-2.19 (m, 1H), 1.72-1.86 (m, 1H), 1.20 (t, *J*=7.14 Hz, 3H).

Step F. Ethyl 5-bromo-8-carbamoyl-9*H*-carbazole-2-carboxylate (30). To a suspension of **29** (60 g, 164 mmol) in THF (400 mL) was added 4,5-dichloro-3,6-dioxocyclohexa-1,4-diene-1,2-dicarbonitrile (78 g, 345 mmol) portion wise at RT. After 1 h, the reaction mixture was added to an aqueous NaOH solution (1N NaOH (500 mL) and water (725 mL)), the resulting suspension filtered and washed with water. The resulting material was dried in vacuo at 50 °C to obtain **30** (51 g, 86%) as a yellow solid. LCMS *m/z* 360.9, 362.9 $(M+H)^+$. ^{1}H NMR (400 MHz, DMSO-d_6) δ 12.00 (s, 1H), 8.69 (d, *J* = 8.4 Hz, 1H), 8.50 (d, *J* = 0.9 Hz, 1H), 8.23 (br s, 1H), 7.92 (d, *J* = 8.1 Hz, 1H), 7.86 (dd, *J* = 8.4, 1.5 Hz, 1H), 7.59 (br s, 1H), 7.50 (d, *J* = 8.1 Hz, 1H), 4.36 (q, *J* = 7.2 Hz, 2H), 1.36 (t, *J* = 7.0 Hz, 3H).

Step G. 5-Bromo-8-carbamoyl-9*H*-carbazole-2-carboxylic acid (34). A solution of **30** (7.2 g, 19.1 mmol) and LiOH monohydrate (1.4 g, 57.2 mmol) in THF/EtOH/H_2O (3:1:1, 201 mL) was heated at reflux for 6 h. The reaction mixture was cooled to RT and concentrated. The resulting residue was suspended in water and the pH was adjusted to ~2-3 with 1N aqueous HCl. The resulting precipitate was collected by filtration, washed with water and dried to provide **34** (7 g, 99%) as an off-white solid. LCMS *m/z* 333, 335 $(M+H)^+$, 316, 318 $(M+H-NH_3)^+$.

Step H. 4-Bromo-7-(4-methylpiperazine-1-carbonyl)-9*H*-carbazole-1-carboxamide (35). A suspension of **34** (7.0 g, 18.9 mmol), EDC (5.1 g, 26.5 mmol), and 1-hydroxybenzotriazole hydrate (4.1 g, 26.5 mmol) in THF/DCM/DMF (378 mL, 4:1:1) was treated with 1-methylpiperazine (6.3 mL, 56.7 mmol). The mixture was stirred at RT overnight, then was concentrated under vacuum. The resulting residue was partitioned between DCM:MeOH (8:1) and saturated aqueous $NaHCO_3$. The aqueous phase was extracted twice again with DCM:MeOH (8:1), and the combined organic phases were washed with brine, dried over Na_2SO_4 and concentrated under vacuum. The resulting residue was suspended in ethyl acetate and allowed to stand overnight, forming a precipitate which was collected by filtration, washed

with ethyl acetate and dried. The filtrates were concentrated under vacuum and the residue was triturated with ethyl acetate-methanol to provide additional precipitate, which was collected by filtration and dried. The process was repeated to yield additional precipitate. The dried precipitates were combined to provide **35** (7.5 g, 96%) as a peach-colored solid. LCMS *m/z* 415, 417 $(M+H)^+$. ^{1}H NMR (400 MHz, DMSO-d_6) δ 11.83 (s, 1H), 8.57 (d, *J*=8.1 Hz, 1H), 8.20 (br s, 1H), 7.84 (d, *J*=8.3 Hz, 1H), 7.79 (s, 1H), 7.56 (br s, 1H), 7.42 (d, *J*=8.1 Hz, 1H), 7.22 (d, *J*=8.1 Hz, 1H), 3.70-3.30 (m, 4H), 2.39-2.20 (m, 4H), 2.16 (s, 3H).

Step I. 2-Methyl-3-(4,4,5,5-tetramethyl-1,3,2-dioxaborolan-2-yl)aniline: A mixture of 3-bromo-2-methylaniline (4.0 g, 21.5 mmol), bis(pinacolato)diboron (6.5 g, 25.8 mmol) and potassium acetate (4.2 g, 43.0 mmol) in 1,4-dioxane (44.8 mL) and DMSO (9 mL) was bubbled with nitrogen for 10 min. $PdCl_2$(dppf)-CH_2Cl_2 adduct (0.53 g, 0.64 mmol) was added and the mixture was degassed for another 5 min, then was heated to reflux. After 2 h, the mixture was cooled to RT, filtered through Celite, and the solids were washed with ethyl acetate. The combined filtrates were washed sequentially with water and brine. The organic phase was dried over Na_2SO_4 and concentrated under vacuum. The resulting residue was purified by chromatography (eluting with ethyl acetate-hexanes, 5:95, then 15:85), to provide 2-methyl-3-(4,4,5,5-tetramethyl-1,3,2-dioxaborolan-2-yl)aniline as an off-white solid (4.4 g, 88%).

Step J. 4-(3-Amino-2-methylphenyl)-7-(4-methylpiperazine-1-carbonyl)-9*H*-carbazole-1-carboxamide (7a). A mixture of **35** (3.0 g, 7.2 mmol), $Pd(Ph_3P)_4$ (0.4 g, 0.36 mmol), 2 M aqueous Na_2CO_3 (9 mL, 18.1 mmol), and 2-methyl-3-(4,4,5,5-tetramethyl-1,3,2-dioxaborolan-2-yl)aniline (2 g, 8.7 mmol) in toluene-ethanol (4:1, 181 mL) under nitrogen was heated at 90 °C for 11 h. The mixture was cooled to RT and treated with water, saturated aqueous $NaHCO_3$ and ethyl acetate. An insoluble gummy solid was formed. The supernatant phases were decanted, and the organic phase was separated and washed with brine. The gummy solid was dissolved in MeOH, combined with the ethyl acetate phase, and the combined solution was dried over Na_2SO_4 and concentrated under vacuum. The residue was suspended in ethyl acetate, forming a precipitate which was collected by filtration, washed with ethyl acetate and dried. Additional solid was isolated from the filtrates, and the combined solids were

triturated with ethyl acetate to provide **7a** (2.45 g, 77%) as a white solid. LCMS *m/z* 442.2 $(M+H)^+$. ^1H NMR (400 MHz, DMSO-d_6) δ 11.65 (s, 1H), 8.19 (br s, 1H), 8.00 (d, *J*=7.9 Hz, 1H), 7.75 (s, 1H), 7.51 (br s, 1H), 7.09-7.01 (m, 1H), 6.98-6.85 (m, 3H), 6.82-6.76 (m, 1H), 6.47 (d, *J*=6.2 Hz, 1H), 5.02 (s, 2H), 3.74-3.22 (m, 4H), 2.29 (s, 4H), 2.18 (s, 3H), 1.71 (s, 3H).

Step K. 4-(3-(4-Fluorobenzamido)-2-methylphenyl)-7-(4-methylpiperazine-1-carbonyl)-9*H*-carbazole-1-carboxamide, TFA (5). To a solution of **7a** (26 mg, 0.059 mmol) and DIEA (0.031 mL, 0.177 mmol) in THF (2 mL) was added 4-fluorobenzoyl chloride (0.014 mL, 0.118 mmol). The reaction mixture was stirred at RT overnight and concentrated. The resulting crude residue was purified by preparative HPLC to give a TFA salt of **5** (23 mg, 59%) as a white solid. LCMS *m/z* 564.3 $(M+H)^+$. ^1H NMR (400 MHz, DMSO-d_6) δ 11.77 (s, 1H), 10.15 (s, 1H), 9.81 (br s, 1H), 8.26 (br s, 1H), 8.14-8.03 (m, 3H), 7.85 (s, 1H), 7.63-7.48 (m, 2H), 7.46-7.32 (m, 3H), 7.22 (d, *J*=7.3 Hz, 1H), 7.08-6.99 (m, 3H), 3.32-2.99 (m, 7H), 2.82 (s, 3H), 1.91 (s, 3H).

7-(2-Hydroxypropan-2yl)-4-(2-methyl-3-(4-oxoquinazolin-3(4*H*)-yl))phenyl-9*H*-carbazole-1-carboxamide (6).

Step A. 4-Bromo-7-(2-hydroxypropan-2-yl)-9*H*-carbazole-1-carboxamide (31). To a solution of **30** in THF (600 mL) at -75 °C was added drop wise 1.6 N methyl lithium solution in hexane (529 mL, 847 mmol). The addition temperature was maintained below -60 °C. There was a heavy yellow suspension observed, requiring the addition of more THF (200 mL) to maintain stirring. The reaction mixture was stirred for 30 min. at -75 °C, then quenched by the slow addition of MeOH (132 mL), followed by 6N HCl (190 mL) to adjust the pH to 2-3. The reaction mixture was allowed to warm to RT and the layers were separated. The acidic aqueous layer was back extracted with EtOAc (300 mL) and both organic layers were combined, washed with saturated $NaHCO_3$ solution, dried over Na_2SO_4, and treated with activated charcoal and stirred for 30 min at RT. The suspension was filtered through Celite, the filtrate concentrated and the resulting residue was triturated with anhydrous ether (250 mL) and stirred for 1 h

at RT. The resulting solid was filtered and dried to give **31** (40 g, 84%). LCMS *m/z* 331 $(M+H-H_2O)^+$. ^1H NMR (400 MHz, DMSO-d_6) δ 11.56 (s, 1H), 8.48 (d, *J*=8.4 Hz, 1H), 8.16 (br s, 1H), 7.93 (d, *J*=1.1 Hz, 1H), 7.80 (d, *J*=8.1 Hz, 1H), 7.57-7.44 (m, 1H), 7.42-7.32 (m, 2H), 5.07 (s, 1H), 1.50 (s, 6H).

Step B. 3-(3-Bromo-2-methylphenyl)quinazolin-4(3*H*)-one (50). A mixture of anthranilic acid (80 g, 583 mmol), 3-bromo-2-methylaniline (109 g, 583 mmol), and triethyl orthoformate (86 g, 583 mmol) in toluene (800 mL) was heated to 85 °C to distill off ethanol. After the distillation was complete, the reaction mixture was refluxed at 110 °C for 16 hours with a Dean-Stark apparatus to collect water. After cooling to RT, the reaction mixture was concentrated and the resulting residue was dissolved in EtOAc (600 mL). The organic layer was washed with saturated $NaHCO_3$ solution, water, dried over Na_2SO_4 and concentrated. The resulting solid was triturated with anhydrous ether for 30 min at RT and collected by filtration to give **50** (115 g, 63%) as an off white solid. LCMS *m/z* 314.0, 316.0 $(M+H)^+$. ^1H NMR (400 MHz, $CDCl_3$) δ 8.38 (dd, *J*=7.9, 0.7 Hz, 1H), 7.97 (s, 1H), 7.94 (dd, *J*=7.2, 1.7 Hz, 1H), 7.85-7.77 (m, 2H), 7.56 (ddd, *J*=8.0, 6.4, 1.9 Hz, 1H), 7.38-7.33 (m, 1H), 7.33-7.29 (m, 1H), 2.37 (s, 3H).

Step C. 3-(2-Methyl-3-(4,4,5,5-tetramethyl-1,3,2-dioxaborolan-2-yl)phenyl)quinazolin-4(3*H*)-one (51). A mixture of **50** (60 g, 190 mmol), $PdCl_2$(dppf)-CH_2Cl_2 adduct (3.9 g, 4.8 mmol), 4,4,4',4',5,5,5',5'-octamethyl-2,2'-bi(1,3,2-dioxaborolane) (53.2 g, 209 mmol), and potassium acetate (56.1 g, 571 mmol) in dioxane (500 mL) was heated to reflux for 1 h. The reaction mixture was cooled to RT and concentrated. The resulting dark residue was dissolved in EtOAc (400 mL), washed twice with water, the organic layer filtered through Celite and dried over Na_2SO_4 with activated charcoal for 30 min at RT. The mixture was filtered through Celite, concentrated and purified in three portions by chromatography (eluting with EtOAc/hexanes, 0-35% gradient) to obtain **51** (45 g, 65%). LCMS *m/z* 363.1 $(M+H)^+$. ^1H NMR (400 MHz, $CDCl_3$) δ 8.38 (dq, *J*=8.0, 0.6 Hz, 1H), 7.96 (s, 1H), 7.94 (dd, *J*=7.2, 1.7 Hz, 1H), 7.86-7.74 (m, 2H), 7.56 (ddd, *J*=8.0, 6.4, 1.9 Hz, 1H), 7.39-7.32 (m, 1H), 7.32-7.29 (m, 1H), 2.37 (s, 3H), 1.35 (s, 12H).

Step D. 7-(2-Hydroxypropan-2yl)-4-(2-methyl-3-(4-oxoquinazolin-3(4*H*)-yl))phenyl-9*H*-carbazole-1-carboxamide (6). To a mixture of **31** (24 g, 69.1 mmol) and **51** (27.5 g, 76 mmol) in toluene (360 mL) and ethanol (120 mL) was added 2 M aqueous K_3PO_4 (104 mL, 208 mmol) and $Pd(PPh_3)_4$ (3.99 g, 3.46 mmol). The reaction mixture was then heated to 75-80 °C for 16 h. After cooling to RT, the precipitated gray solid was collected by filtration, was suspended in THF (120 mL) and heated at 65 °C for 2 h. After cooling to RT, the dark solution was filtered through Celite to remove Pd material. The filtrate was divided into 3 equal portions and purified by chromatography (eluting with MeOH-DCM, 2-7% gradient) to give **6** (18 g, 52%) as a colorless solid, and as a mixture of four atropisomers. CHN analysis, Calcd for $C_{31}H_{26}N_4O_3$ $0.79H_2O$: C, 72.04, H, 5.38, N, 10.84, H_2O, 2.76; Found: C, 72.27, H, 5.25, N, 10.88, H_2O, 2.76; Pd 27 ppm. LCMS *m/z* 503.0 $(M+H)^+$. ^1H NMR (500 MHz, DMSO-d6) δ 11.43 (s, 0.6H), 11.42 (s, 0.4H), 8.48 (s, 0.4H), 8.41 (s, 0.6H), 8.26 (dd, *J*=8.04, 1.22 Hz, 0.4H), 8.23 (dd, *J*=8.04, 1.22 Hz, 0.6H), 8.15 (br s, 2H), 8.00 (d, *J*=7.79 Hz, 0.4H), 7.99 (d, *J*=7.79 Hz, 0.6H), 7.88-7.92 (m, 1H), 7.86 (dd, *J*=7.91, 1.10 Hz, 1H), 7.79 (d, *J*=5.11 Hz, 0.6H), 7.77 (d, *J*=5.36 Hz, 0.4H), 7.62-7.67 (m, 1H), 7.60 - 7.62 (m, 1H), 7.58 (t, *J*=7.30 Hz, 1H), 7.48 (dd, *J*=7.55, 1.22 Hz, 0.4H), 7.46 (dd, *J*=7.43, 1.10 Hz, 0.6H), 7.12-7.14 (m, 0.4H), 7.11 (dd, *J*=5.84, 1.70 Hz, 0.6H), 7.06 (d, *J*=8.28 Hz, 0.6H), 7.03 (d, *J*=7.79 Hz, 0.4H), 7.00 (d, *J*=7.79 Hz, 0.6H), 6.85 (d, *J*=8.52 Hz, 0.4H), 5.00 (s, 0.6H), 4.97 (s, 0.4H), 1.79 (s, 1.5H), 1.76 (s, 1.5H), 1.47 (d, J=4.38 Hz, 3H), 1.46 (d, J=1.22 Hz, 3H). ^{13}C NMR (126 MHz, DMSO-d6) δ 169.00, 168.97, 159.80, 159.78, 148.89 (s, 2C), 147.94 (s, 2C), 147.34, 147.29, 141.51 (s, 2C), 140.36 (s, 2C), 139.01, 138.96, 137.81, 137.70, 137.42, 137.24, 134.75, 134.70, 134.00, 133.56, 130.21, 130.13, 128.19, 128.08, 127.52, 127.50, 127.43, 127.39, 127.18, 127.08, 126.48, 126.40, 124.13, 124.03, 121.88, 121.84, 121.80, 121.62, 120.42, 119.94, 119.07, 119.02, 118.48, 118.37, 116.88, 116.60, 114.97, 114.93, 108.01, 107.87, 70.94, 70.92, 32.39, 32.27, 32.12, 32.05, 14.55, 14.48. Numerous carbons were split due to the diastereomeric nature of the mixture of atropisomers.

4-(3-(5-Fluoropicolinamido)-2-methylphenyl)-7-(4-methylpiperazine-1-carbonyl)-9*H*-carbazole-1-carboxamide (10). A mixture of **7a** (100 mg, 0.2 mmol), 5-fluoropicolinic acid (43.1 mg, 0.31 mmol),

and 1-hydroxy-7-azabenzotriazole (41.6 mg, 0.31 mmol) in acetonitrile (2 mL) was treated with diisopropylethylamine (0.053 mL, 0.31 mmol) and EDC (78 mg, 0.41 mmol). After 18 h at RT, the mixture was diluted with methanol and purified by preparative HPLC (Phenomenex AXIA C_{18} 21.2 x 100 mm, 5-95% methanol-water containing 0.1% TFA, 10 min, 20 mL/min, 220 nm). The aqueous residue from partial concentration of the appropriate effluent fractions was made basic with saturated aqueous $NaHCO_3$ and extracted with ethyl acetate (3x). The combined organic phases were dried over Na_2SO_4 and concentrated under vacuum to provide **10** as a light gray powder (111.5 mg, 92%). LCMS *m/z* 565.2 $(M+H)^+$. ^{1}H NMR (400 MHz, CD_3OD) δ 8.58 (d, *J*=3.1 Hz, 1H) 8.31 (dd, *J*=8.8, 4.8 Hz, 1H) 7.96 - 8.03 (m, 2H) 7.82 (td, *J*=8.6, 2.6 Hz, 1H) 7.68 (d, *J*=0.9 Hz, 1H) 7.45 (t, *J*=7.9 Hz, 1H) 7.23 (dd, *J*=7.5, 0.9 Hz, 1H) 7.09 (d, *J*=7.9 Hz, 1H) 7.03-7.08 (m, 1H) 6.95-7.00 (m, 1H) 3.78 (br s, 2H) 3.49 (br s, 2H) 2.52 (br s, 2H) 2.40 (br s, 2H) 2.31 (s, 3H) 2.04 (s, 3H). Contains 0.33 equiv. (5% by weight) residual ethyl acetate.

4-(3-(4-Fluorobenzamido)-2-methylphenyl)-7-(isopropylamino)-9*H*-carbazole-1-carboxamide (11).

Step A. Benzyl 5-bromo-8-carbamoyl-9*H*-carbazol-2-yl-carbamate (36). To a suspension of **34** (4.6 g, 12.6 mmol) and 4Å molecular sieves (4.6 g) in 1,4-dioxane (126 mL) at 50 °C was added Et_3N (4.3 mL, 31 mmol) and diphenylphosphoryl azide (6.7 mL, 31 mmol). The mixture was stirred at 50 ^{o}C for 1.5 h at which point phenylmethanol (13 mL, 126 mmol) was added, and the reaction temperature was increased to 85 °C. After 18 h, the reaction mixture was cooled to RT, filtered through Celite, the solid washed with MeOH, EtOAc, and acetone. The filtrates were concentrated to afford crude **36** as a light brown syrup. The syrup was triturated with MeOH, the resulting solid collected by filtration, washed with MeOH, and dried. The resulting filtrates were concentrated, triturated with MeOH again, and the solid collected by filtration. The pale solids were combined to give **36** (5.1 g, 91%). LCMS *m/z* 437.9, 439.9 $(M+H)^+$. ^{1}H NMR (400 MHz, DMSO-d_6) δ 11.63 (s, 1H), 9.98 (s, 1H), 8.43 (d, *J*=8.6 Hz, 1H), 8.16 (br s, 1H), 8.06 (s, 1H), 7.76 (d, *J*=8.3 Hz, 1H), 7.60-7.23 (m, 8H), 5.19 (s, 2H).

Step B. Benzyl 5-(3-amino-2-methylphenyl)-8-carbamoyl-9*H*-carbazol-2-ylcarbamate. A suspension of **36** (1 g, 2.3 mmol), $(Ph_3P)_4Pd$ (0.13 g, 0.11 mmol), 2 M aqueous Na_2CO_3 (2.8 mL, 5.7

mmol), and 2-methyl-3-(4,4,5,5-tetramethyl-1,3,2-dioxaborolan-2-yl)aniline (0.64 g, 2.7 mmol) in toluene/EtOH (4/1) (57 mL) under nitrogen was heated at 90 ^{o}C for 10 h. After cooling to RT, the reaction mixture was filtered through Celite, which was washed with EtOAc. The filtrates were partitioned between EtOAc and water, the organic phase washed with brine, dried over Na_2SO_4, and concentrated to afford a yellow colored solid. The crude product was triturated with MeOH to give benzyl 5-(3-amino-2-methylphenyl)-8-carbamoyl-9*H*-carbazol-2-ylcarbamate as an off-white solid (0.86 g in 82%). LCMS *m/z* 465.1 $(M+H)^+$. ^{1}H NMR (400 MHz, DMSO-d_6) δ 11.47 (s, 1H), 9.82 (s, 1H), 8.14 (br s, 1H), 7.97 (d, *J*=1.3 Hz, 1H), 7.91 (d, *J*=7.5 Hz, 1H), 7.47 (br s, 1H), 7.45-7.31 (m, 5H), 7.30-7.24 (m, 1H), 7.17 (d, *J*=7.5 Hz, 1H), 6.97-6.86 (m, 3H), 6.67 (d, *J*=8.8 Hz, 1H), 5.15 (s, 2H), 1.84 (s, 3H) (some exchangeable protons diffuse and not observed).

Step C. Benzyl 8-carbamoyl-5-(3-(4-fluorobenzamido)-2-methylphenyl)-9*H*-carbazol-2-ylcarbamate. To a mixture of benzyl 5-(3-amino-2-methylphenyl)-8-carbamoyl-9*H*-carbazol-2-ylcarbamate (700 mg, 1.5 mmol) and Hunig's Base (1 mL, 6 mmol) in THF (80 mL) at RT was added 4-fluorobenzoyl chloride (0.36 mL, 3 mmol). After 1 hr the reaction mixture was concentrated, then partitioned between DCM, water, and sat. $NaHCO_3$. The organic phases were separated, washed with brine, dried over Na_2SO_4, and concentrated. The resulting residue was purified by chromatography (eluting with hexane/EtOAc, 70/30 - 50/50 - 30/70) to give benzyl 8-carbamoyl-5-(3-(4-fluorobenzamido)-2-methylphenyl)-9H-carbazol-2-ylcarbamate (721 mg, 82%) as an off-white foamy solid. LCMS *m/z* 587.3 $(M+H)^+$. ^{1}H NMR (400 MHz, DMSO-d_6) δ 11.47 (s, 1H), 10.13 (s, 1H), 9.82 (s, 1H), 8.08 (dd, *J*=9.0, 5.5 Hz, 2H), 7.98 (d, *J*=1.3 Hz, 1H), 7.93 (d, *J*=7.7 Hz, 1H), 7.50-7.33 (m, 11H), 7.20 (dd, *J*=7.5, 1.1 Hz, 1H), 6.95 (d, *J*=7.7 Hz, 2H), 6.79 (d, *J*=8.8 Hz, 1H), 5.16 (s, 2H), 1.89 (s, 3H).

Step D. 7-Amino-4-(3-(4-fluorobenzamido)-2-methylphenyl)-9*H*-carbazole-1-carboxamide (9a). A suspension of benzyl 8-carbamoyl-5-(3-(4-fluorobenzamido)-2-methylphenyl)-9*H*-carbazol-2-ylcarbamate (720 mg, 1.2 mmol) in hydrogen bromide in acetic acid (2.45 mL, 12.3 mmol) was stirred at RT for 1 h. To the above suspension was added EtOAc, water, and 1 M NaOH to give a basic aqueous layer (pH ~9). The organic phases were washed with brine, dried over Na_2SO_4, filtered, and

concentrated. The crude product was then triturated with EtOAc to give 7-amino-4-(3-(4-fluorobenzamido)-2-methylphenyl)-9*H*-carbazole-1-carboxamide (**9a**) (0.33 g, 59%) as a greenish-yellow solid. LCMS *m/z* 453.0 $(M+H)^+$. ^{1}H NMR (400 MHz, DMSO-d_6) δ 11.02 (s, 1H), 10.11 (s, 1H), 8.09 (dd, *J*=8.8, 5.3 Hz, 3H), 7.78 (d, *J*=7.9 Hz, 1H), 7.48-7.43 (m, 1H), 7.42-7.32 (m, 4H), 7.18 (dd, *J*=7.5, 0.9 Hz, 1H), 6.89-6.75 (m, 2H), 6.60 (d, *J*=8.8 Hz, 1H), 6.21 (dd, *J*=8.6, 2.0 Hz, 1H), 5.18 (s, 2H), 1.90 (s, 3H).

Step E. 4-(3-(4-Fluorobenzamido)-2-methylphenyl)-7-(isopropylamino)-9*H*-carbazole-1-carboxamide (11). A suspension of 7-amino-4-(3-(4-fluorobenzamido)-2-methylphenyl)-9*H*-carbazole-1-carboxamide (30 mg, 0.066 mmol), acetone (0.019 mL, 0.265 mmol), and sodium triacetoxyborohydride (35.1 mg, 0.166 mmol) in DCM/THF (3 mL, 2/1) was stirred at RT overnight. After 18 h, the reaction mixture was concentrated, dissolved in DMF, and purified by prep HPLC to give **11** (11 mg, 24%) as a pale solid. LCMS *m/z* 495.0 $(M+H)^+$. ^{1}H NMR (500 MHz, CD_3OD) δ 8.12-8.01 (m, 3H), 7.66 (d, *J*=1.4 Hz, 1H), 7.55-7.50 (m, 1H), 7.46 (t, *J*=7.8 Hz, 1H), 7.33-7.20 (m, 4H), 7.15 (d, *J*=7.8 Hz, 1H), 6.97 (dd, *J*=8.6, 1.9 Hz, 1H), 3.80 (dt, *J*=13.0, 6.5 Hz, 1H), 1.99 (s, 3H), 1.35 (dd, *J*=6.2, 5.1 Hz, 6H).

4-(2-Methyl-3-(1-oxoisoindolin-2-yl)phenyl)-7-(4-methylpiperazine-1-carbonyl)-9*H*-carbazole-1-carboxamide (12).

Step A. 2-(3-Bromo-2-methylphenyl)isoindolin-1-one (39a). To a solution of 3-bromo-2-methylaniline (2 g, 10.8 mmol) in DCM (25 mL) and TEA (3 mL, 21.5 mmol) at RT was slowly added a DCM (10 mL) solution of 2-(chloromethyl)benzoyl chloride (2 g, 10.8 mmol) over 1.5 h. The reaction mixture was then washed with water and brine, and concentrated to give *N*-(3-bromo-2-methylphenyl)-2-(chloromethyl)benzamide as a tan solid. A 60% oil dispersion of NaH (0.86 g, 21.5 mmol) was washed twice with hexanes and suspended in tetrahydrofuran (25 mL). To this suspension was slowly added a THF (50 mL) solution of *N*-(3-bromo-2-methylphenyl)-2-(chloromethyl)benzamide. After the addition was complete the mixture was stirred at RT for 1 h. The reaction mixture was then

diluted with DCM and quenched carefully with methanol, washed with water, brine and concentrated to give **39a** (1.9 g, 60%) as a tan solid. LCMS *m/z* $(M+H)^+$ 301.9, 303.9.

Step B. 2-(2-Methyl-3-(4,4,5,5-tetramethyl-1,3,2-dioxaborolan-2-yl)phenyl)isoindolin-1-one (40a). Nitrogen was bubbled into a mixture of **39a** (1.5 g, 5 mmol), 4,4,4',4',5,5,5',5'-octamethyl-2,2'-bi(1,3,2-dioxaborolane) (1.9 g, 7.4 mmol), and potassium acetate (1.5 g, 14.9 mmol) in dioxane (40 mL) for 10 min, followed by the addition of PdCl2(dppf)-CH_2Cl_2 adduct (0.12 g, 0.15 mmol). The resulting mixture was heated to reflux for 4 h and diluted with ethyl acetate. The resulting mixture was filtered, the filtrate washed with water and again filtered. The resulting solution was concentrated and the residue purified by chromatography (eluting with EtOAc/hexane, 10-50% gradient) to give **40a** (1.2 g, 69%) as a light yellow sticky foam. LCMS *m/z* $(M+H)^+$ 350.1.

Step C. 4-(2-Methyl-3-(1-oxoisoindolin-2-yl)phenyl)-7-(4-methylpiperazine-1-carbonyl)-9H-carbazole-1-carboxamide (12). To a mixture of **35** (52 mg, 0.12 mmol) and **40a** (52 mg, 0.15 mmol) in toluene (3 mL) and ethanol (1 mL) was added 2 M aqueous K_3PO_4 (0.19 mL, 0.38 mmol) and then $Pd(Ph_3P)_4$ (7.2 mg, 6.3 μmol). The reaction mixture was heated at 100 °C for 8 h and then diluted with ethyl acetate. The mixture was washed with water and the organic layer concentrated. The resulting residue was purified by chromatography (eluting with 90:9:1 DCM:MeOH:NH_4OH/DCM, 50-100% gradient) to give **12** (44 mg), which was further purified by prep HPLC (Phenomenex Luna Axia, 5μ, 21x100 mm, solvent A: 10% MeOH- 90% H_2O- 0.1% TFA; solvent B: 90% MeOH- 10% H_2O- 0.1% TFA, gradient: 0-100% B, gradient time: 10 min, flow rate: 30 ml/min, wavelength 220 nm) to give **12** (30 mg, 44%) as a white solid. LCMS *m/z* $(M+H)^+$ 558.2; ^{1}H NMR (400 MHz, $CDCl_3$) δ 10.68 (s, 1 H), 7.97 (d, *J*=8.35 Hz, 1H), 7.70 (d, *J*=7.47 Hz, 1H), 7.63 (t, *J*=6.81 Hz, 1H), 7.51-7.58 (m, 3H), 7.46 (d, *J*=3.95 Hz, 2H), 7.33-7.39 (m, 1H), 7.08-7.16 (m, 3H), 4.83 (s, 2H), 3.30-4.04 (m, 4H), 2.34-2.61 (m, 4H), 2.32 (s, 3H), 1.93 (s, 3H) (some exchangeable protons diffuse and not observed).

7-(2-Hydroxypropan-2-yl)-4-(2-methyl-3-(1-oxoisoindolin-2-yl)phenyl)-9*H*-carbazole-1-carboxamide (13). A mixture of **31** (40 mg, 0.12 mmol), **40a** (40 mg, 0.12 mmol), $Pd(Ph_3P)_4$ (6.7 mg, 5.8 umol) and 2 M aqueous K_3PO_4 (0.14 mL, 0.28 mmol) in toluene (2 mL) and EtOH (0.5 mL) was

heated at 90 °C for 16 h. After cooling to RT, the reaction mixture was diluted with DMF (1 mL), filtered and purified by preparative HPLC. The product containing fractions were collected, basified with 1N NaOH and extracted twice with DCM. The combined organic phases were washed with water and concentrated. The resulting residue was purified further by chromatography (eluting with a gradient from 100% DCM to 0.8:7.2:92 ammonia-MeOH-DCM) to give **13** as a white solid (25 mg, 42%). Mass spectrum *m/z* 472.2 $(M\text{-}OH)^+$. ^1H NMR (400 MHz, CD_3OD) δ 7.95 (d, *J*=7.92 Hz, 1H), 7.89 (d, *J*=7.48 Hz, 1H), 7.76 (d, *J*=1.10 Hz, 1H), 7.65-7.73 (m, 2H), 7.48 - 7.61 (m, 3H), 7.41 (dd, *J*=7.04, 1.76 Hz, 1H), 7.17 (dd, *J*=8.36, 1.54 Hz, 1H), 7.04-7.10 (m, 2H), 4.96 (s, 2H), 1.92 (s, 3H), 1.61 (d, *J*=3.74 Hz, 6H).

4-(3-(6-Fluoro-1-oxoisoindolin-2-yl)-2-methylphenyl)-7-(2-hydroxypropan-2-yl)-9*H*-carbazole-1-carboxamide (14).

Step A. *N*-(3-Bromo-2-methylphenyl)-2-(bromomethyl)-5-fluorobenzamide. To a solution of 2-(bromomethyl)-5-fluorobenzoic acid (3.1 g, 13.1 mmol) in DCM (50 mL) at RT was added 6 drops of DMF and oxalyl dichloride (1.7 g, 13.1 mmol). After 1 h, the reaction was concentrated, redissolved in DCM and concentrated again. The resulting residue was redissolved in DCM (50 mL) and 3-bromo-2-methylaniline (1.7 g, 9.1 mmol) was added. After stirring for 1 h, Et_3N (2.9 mL, 15.7 mmol) was added portion-wise. The reaction mixture was diluted with DCM (100 mL) after 2 h, the organic layer washed with satd. $NaHCO_3$, water, and concentrated. The resulting solid residue was triturated with DCM to give *N*-(3-bromo-2-methylphenyl)-2-(bromomethyl)-5-fluorobenzamide (1.4 g). The mother liquor was purified by chromatography (eluting with ethyl acetate/hexane, 0-70% gradient) to give additional material (2.5 g total, 48%) suitable for the subsequent reaction.

Step B. 2-(3-Bromo-2-methylphenyl)-6-fluoroisoindolin-1-one (39b). A mixture of *N*-(3-bromo-2-methylphenyl)-2-(bromomethyl)-5-fluorobenzamide (2.5 g, 6.3 mmol) and sodium *tert*-butoxide (0.91 g, 9.5 mmol) in THF (80 mL) was stirred at RT for 30 min. The reaction mixture was quenched with water, extracted with DCM twice, the combined organic phases washed with water and concentrated.

The resulting residue was purified by chromatography (eluting with hexane/ethyl acetate) to give **39b** (1.18 g, 59%) as a white solid. LCMS *m/z* $(M+H)^+$ 319.9, 321.9.

Step C. 6-Fluoro-2-(2-methyl-3-(4,4,5,5-tetramethyl-1,3,2-dioxaborolan-2-yl)phenyl)isoindolin-1-one (40b). A solution of **39b** (1.3 g, 4.1 mmol), 4,4,4',4',5,5,5',5'-octamethyl-2,2'-bi(1,3,2-dioxaborolane) (1.6 g, 6.1 mmol), $PdCl_2$(dppf)-CH_2Cl_2 adduct (0.17 g, 0.2 mmol), and potassium acetate (1.2 g, 12.2 mmol) in dioxane (20 mL) was heated at 90 °C overnight. The reaction mixture was diluted with DCM, washed with water, the organic layer separated, and the aqueous layer was extracted twice more with DCM. The combined organic extracts were concentrated and the crude material was purified by chromatography (eluting with EtOAc/hexane, 0-50% gradient) to give **40b** (1.35 g, 86%) as a white solid. LCMS *m/z* $(M+H)^+$ 368.0. ^{1}H NMR (400 MHz, $CDCl_3$) δ 7.82 (dd, *J*=6.93, 1.87 Hz, 1H), 7.63 (dd, *J*=7.59, 2.31 Hz, 1H), 7.47 (dd, *J*=8.25, 4.29 Hz, 1H), 7.27-7.34 (m, 3H), 4.65 (s, 2H), 2.41 (s, 3H), 1.32-1.37 (m, 12H).

Step D. 4-(3-(6-Fluoro-1-oxoisoindolin-2-yl)-2-methylphenyl)-7-(2-hydroxypropan-2-yl)-9*H*-carbazole-1-carboxamide (14). A mixture of **31** (30 mg, 0.09 mmol), **40b** (41 mg, 0.11 mmol), $Pd(Ph_3P)_4$ (5 mg, 4.3 μmol), and 2 M aqueous K_3PO_4 (0.13 mL, 0.26 mmol) in toluene (3 mL) and ethanol (1 mL) was heated at 100 °C for 9 h. The reaction mixture was cooled to RT, partitioned between water and ethyl acetate, and the organics concentrated to give yellow solid. The crude material was purified by chromatography (eluting with 90:9:1 DCM:MeOH:NH_4OH/DCM, 10-30% gradient) to give **14** (28 mg, 59%) as a white solid. LCMS *m/z* $(M+H- H_20)^+$ = 490.3. ^{1}H NMR (400 MHz, $CDCl_3$) δ 10.60 (s, 1H), 7.70 (d, *J*=1.10 Hz, 1H), 7.63-7.68 (m, 2H), 7.52 (dd, *J*=8.36, 4.40 Hz, 1H), 7.44-7.48 (m, 2H), 7.31-7.41 (m, 2H), 7.21 (dd, *J*=8.36, 1.76 Hz, 1H), 7.06-7.11 (m, 2H), 4.82 (s, 2H), 2.01 (s, 1H), 1.97 (s, 3H), 1.66 (s, 6H) (some exchangeable protons diffuse and not observed).

7-(2-Hydroxypropan-2-yl)-4-(2-methyl-3-(1-oxo-3,4-dihydroisoquinolin-2(1*H*)-yl)phenyl)-9*H*-carbazole-1-carboxamide (15).

Step A. 7-(2-Hydroxypropan-2-yl)-4-(4,4,5,5-tetramethyl-1,3,2-dioxaborolan-2-yl)-9*H*-carbazole-1-carboxamide (33). A mixture of **31** (5 g, 14.4 mmol), 4,4,4',4',5,5,5',5'-octamethyl-2,2'-bi(1,3,2-

dioxaborolane) (4.4 g, 17.3 mmol), potassium acetate (4.2 g, 43.2 mmol) and $PdCl_2$(dppf)-CH_2Cl_2 adduct (0.59 g, 0.72 mmol) was equally divided into two large pressure reaction vials, suspended in dioxane (30 mL), sealed and heated at 110 °C for 4.5 h. The two reaction mixtures were then combined, diluted with ethyl acetate, washed with water, filtered through Celite and concentrated. The resulting black residue was purified by chromatography (eluting with EtOAc/hexane, 50-100% gradient) to give **33** (3.9 g, 67%). LCMS *m/z* 376.9 $(M+H-OH)^+$. ^1H NMR (400 MHz, $CDCl_3$) δ 10.55 (br s, 1H), 8.92 (d, *J*=8.6 Hz, 1H), 7.71 (d, *J*=7.7 Hz, 1H), 7.59-7.52 (m, 2H), 7.43 (dd, *J*=8.5, 1.7 Hz, 1H), 1.49 (s, 12H) (some exchangeable protons diffuse and not observed).

Step B. 3,4-Dihydroisoquinolin-l (2*H*)-one (46). A solution of 2,3-dihydro-1*H*-inden-1-one (1 g, 7.6 mmol) in DCM (10 mL) was treated with methane sulfonic acid (10 mL) and cooled to 0 °C. Sodium azide (0. 98 g, 15.1 mmol) was added and the mixture was stirred at 0 °C for 2 h, then at RT overnight. The mixture was made basic with 20% aqueous sodium hydroxide and extracted with DCM. The organic phase was washed with water, dried and concentrated. The resulting residue was purified by chromatography (eluting with hexane-EtOAc) to provide 3,4-dihydroisoquinolin-l (2*H*)-one **46** as a colorless oil (162 mg, 15%). Mass spectrum m/z 148.1 $(M+H)^+$. 1H NMR (400 MHz, CD3OD) δ 7.93 (dd, *J*=7.8, 1.0 Hz, 1H), 7.44-7.52 (m, 1H), 7.35 (td, *J*=7.6, 1.2 Hz, 1H), 7.29 (d, *J*=7.7 Hz, 1H), 3.50 (t, *J*=6.6 Hz, 2H), 2.98 (t, *J*=6.7 Hz, 2H).

Step C. 2-(3-Bromo-2-methylphenyl)-3,4-dihydroisoquinolin-1(2*H*)-one (47). A mixture of 1,3-dibromo-2-methylbenzene (340 mg, 1.36 mmol), 46 (100 mg, 0.68 mmol) and potassium carbonate (94 mg, 0.68 mmol) in DMSO (2 mL) was purged with nitrogen, treated with copper (I) iodide (26 mg, 0.14 mmol) and heated at 150 °C for 3.5 h. The mixture was combined with that from a second identical reaction using 1, 3-dibromo-2-methylbenzene (2.6 g, 10.4 mmol) and 3, 4-dihydroisoquinolin-l (2*H*)-one (508 mg, 3.4 mmol), diluted with DCM and filtered through Celite. The filtrate was washed with 5% aqueous ammonium hydroxide, dried and concentrated. The residue was purified by chromatography (eluting with hexane-EtOAc) to provide **47** as a yellow solid (142 mg, 11%). Mass spectrum m/z 315.9, 317.9 $(M+H)^+$. 1H NMR (400 MHz, $CDCl_3$) δ 8. 15 (dd, *J*=7.70, 1.10 Hz, 1H), 7.

55 (dd, *J*=7. 92, 1.10 Hz, 1H), 7.46-7.51 (m, 1H), 7.37-7.42 (m, 1H), 7.24-7.28 (m, 1H), 7.17-7.21 (m, 1H), 7.09-7.16 (m, 1H), 3.95 (ddd, *J*=12.21, 10.12, 4.73 Hz, 1H), 3.73 (ddd, *J*=11.94, 6.33, 5.28 Hz, 1H), 3.26 (ddd, *J*=15.74, 10.23, 5.28 Hz, 1H), 3. 06-3. 14 (m, 1H), 2.36 (s, 3H).

Step D. 7-(2-Hydroxypropan-2-yl)-4-(2-methyl-3-(1-oxo-3,4-dihydroisoquinolin-2(1*H*)-yl)phenyl)-9*H*-carbazole-1-carboxamide (15). A mixture of **33** (40 mg, 0.1 mmol), **47** (38 mg, 0.12 mmol), $Pd(Ph_3P)_4$ (5.9 mg, 5 umol) and 2 M aqueous K_3PO_4 (0.13 mL, 0.25 mmol) was heated at 90 °C for 16 h. The reaction mixture was diluted with DCM, washed with water, separated and the organic phase was concentrated. The resulting residue was purified twice by chromatography, and then purified further by prep. HPLC to give **15** (21 mg, 39%) as a white solid. Mass spectrum *m/z* 504.1 $(M+H)^+$. ^1H NMR (400 MHz, $CDCl_3$) δ 10.47-10.59 (m, 1H), 8.13-8.22 (m, 1H), 7.60-7.71 (m, 2H), 7.35-7.53 (m, 4H), 7.28-7.35 (m, 2H), 7.10-7.15 (m, 1H), 6.86-7.07 (m, 1H), 4.06-4.16 (m, 1H), 3.79-3.89 (m, 1H), 3.22-3.34 (m, 1H), 3.08-3.19 (m, 1H), 1.99-2.05 (m, 3H), 1.61-1.67 (m, 6H) (some exchangeable protons diffuse and not observed).

7-(2-Hydroxypropan-2-yl)-4-(2-methyl-3-(1-oxoisoquinolin-2(1*H*)-yl)phenyl)-9*H*-carbazole-1-carboxamide (16).

Step A. 2-(3-Bromo-2-methylphenyl)isoquinoline-1,3(2*H*,4*H*)-dione. A mixture of 3-bromo-2-methylaniline (1 g, 5.4 mmol) and isochroman-1,3-dione (0.87 g, 5.4 mmol) in acetic acid (15 mL) was heated overnight at 100 °C. The solution was cooled to RT, concentrated and purified by chromatography (eluting with EtOAc/hexane, 20-100% gradient) to give 2-(3-bromo-2-methylphenyl)isoquinoline-1,3(2*H*,4*H*)-dione (630 mg, 36%) as a tan solid. LCMS *m/z* $(M+H)^+$ 330.1, 332.1.

Step B. 2-(3-Bromo-2-methylphenyl)-3-hydroxy-3,4-dihydroisoquinolin-1(2*H*)-one. A suspension of 2-(3-bromo-2-methylphenyl)isoquinoline-1,3(2*H*,4*H*)-dione (630 mg, 1.9 mmol) in methanol (100 mL) at RT was treated with $NaBH_4$ (caplets) (217 mg, 5.7 mmol). After 2 h, additional $NaBH_4$ (120 mg) was added. After 4 h, the reaction mixture was concentrated and partitioned between DCM and water. The organic layer was concentrated to give 2-(3-bromo-2-methylphenyl)-3-hydroxy-3,4-

dihydroisoquinolin-1(2*H*)-one (600 mg, 95%) as a light-yellow foam suitable for the subsequent reaction. LCMS *m/z* $(M+H)^+$ 332.1, 334.1.

Step C. 2-(3-bromo-2-methylphenyl)isoquinolin-1(2*H*)-one (43). A solution of 2-(3-bromo-2-methylphenyl)-3-hydroxy-3,4-dihydroisoquinolin-1(2*H*)-one (600 mg, 1.81 mmol) in DCM (30 mL) was treated with TFA (1.4 mL, 18.1 mmol). After 2 h, the reaction mixture was concentrated. The resulting residue was dissolved in DCM, washed with aqueous sodium bicarbonate and water, and the organic layer concentrated. The residue was purified by chromatography (eluting with EtOAc/hexane, 20-60% gradient) to give **43** (380 mg, 67%) as a white solid. LCMS *m/z* $(M+H)^+$ 314.0, 316.0.

Step D. 2-(2-methyl-3-(4,4,5,5-tetramethyl-1,3,2-dioxaborolan-2-yl)phenyl)isoquinolin-1(2*H*)-one (44). A mixture of **43** (360 mg, 1.2 mmol), 4,4,4',4',5,5,5',5'-octamethyl-2,2'-bi(1,3,2-dioxaborolane) (320 mg, 1.3 mmol), potassium acetate (337 mg, 3.4 mmol), and PdCl2(dppf)-CH_2Cl_2 adduct (47 mg, 0.06 mmol) in dioxane (7 mL) was heated at 100 °C for 16 h. The reaction mixture was diluted with ethyl acetate, washed with water, and the organic layer filtered through Celite and concentrated. The black colored residue was purified by chromatography (eluting with EtOAc/hexane, 10-60% gradient) to give **44** (280 mg, 68%) as a white solid. LCMS *m/z* $(M+H)^+$ 362.2.

Step E. 7-(2-Hydroxypropan-2-yl)-4-(2-methyl-3-(1-oxoisoquinolin-2(1*H*)-yl)phenyl)-9*H*-carbazole-1-carboxamide (16). A mixture of **31** (50 mg, 0.14 mmol) and **44** (68 mg, 0.19 mmol) in toluene (3 mL) and ethanol (1 mL) was treated with 2 M aqueous K_3PO_4 (0.22 mL, 0.43 mmol) and $Pd(Ph_3P)_4$ (8.3 mg, 7.2 μmol) and heated at 100 °C for 7 h. The reaction mixture was diluted with ethyl acetate, washed with water and the organic layer concentrated. The resulting residue was purified by chromatography (eluting with EtOAc), followed by further chromatography (eluting with 90:9:1 DCM:MeOH:NH_4OH/DCM, 10-50% gradient) to give **16** (18 mg, 44%) as a white solid and as a mixture of atropisomers. LCMS *m/z* $(M+H)^+$ 502.3. ^1H NMR (400 MHz, $CDCl_3$) δ 10.53-10.64 (m, 1H), 8.52 (d, *J*=8.14 Hz, 1H), 7.41-7.75 (m, 7H), 7.30-7.33 (m, 1H), 7.16-7.21 (m, 2H), 7.04-7.13 (m, 1H), 6.95 (d, *J*=8.36 Hz, 1H), 6.64 (dd, *J*=14.08, 7.48 Hz, 1H), 1.89 (d, *J*=7.92 Hz, 3H), 1.66 (d, *J*=2.86

Hz, 6H) (some exchangeable protons diffuse and not observed). Analytical HPLC showed 87-90% purity.

4-(3-(5-Fluoro-4-oxoquinazolin-3(4*H*)-yl)-2-methylphenyl)-7-(2-hydroxypropan-2-yl)-9*H*-carbazole-1-carboxamide (17).

Step A. 3-(3-Bromo-2-methylphenyl)-5-fluoroquinazolin-4(3*H*)-one. A mixture of 5-fluoro-1*H*-benzo[d][1,3]oxazine-2,4-dione (250 mg, 1.38 mmol), 3-bromo-2-methylaniline (257 mg, 1.38 mmol), and trimethoxymethane (439 mg, 4.14 mmol) in THF (2 mL) was heated at 100 °C for 15 h. The reaction mixture was concentrated and purified by chromatography (eluting with EtOAc/hexane, 10-40% gradient) to yield a yellow solid that was triturated with hexanes to give 3-(3-bromo-2-methylphenyl)-5-fluoroquinazolin-4(3*H*)-one (200 mg, 44%) as a white solid. LCMS *m/z* $(M+H)^+$ 333.1, 335.1.

Step B. 5-Fluoro-3-(2-methyl-3-(4,4,5,5-tetramethyl-1,3,2-dioxaborolan-2-yl)phenyl)quinazolin-4(3*H*)-one.

A mixture of 3-(3-bromo-2-methylphenyl)-5-fluoroquinazolin-4(3*H*)-one (200 mg, 0.6 mmol), 4,4,4',4',5,5,5',5'-octamethyl-2,2'-bi(1,3,2-dioxaborolane) (230 mg, 0.9 mmol), potassium acetate (177 mg, 1.8 mmol), and $PdCl_2$(dppf)-CH_2Cl_2 adduct (25 mg, 0.03 mmol) in dioxane (4 mL) was heated at 100 °C for 3 h. The reaction mixture was diluted with ethyl acetate, the organics washed with water, filtered through Celite and concentrated. The resulting black residue was purified by chromatography (eluting with EtOAc/hexane, 20-40% gradient) to give 5-fluoro-3-(2-methyl-3-(4,4,5,5-tetramethyl-1,3,2-dioxaborolan-2-yl)phenyl)-quinazolin-4(3*H*)-one (170 mg, 75%) as a white foam. LCMS *m/z* $(M+H)^+$ 381.3.

Step C. 4-(3-(5-Fluoro-4-oxoquinazolin-3(4*H*)-yl)-2-methylphenyl)-7-(2-hydroxypropan-2-yl)-9*H*-carbazole-1-carboxamide (17). A mixture of **31** (35 mg, 0.1 mmol), 5-fluoro-3-(2-methyl-3-(4,4,5,5-tetramethyl-1,3,2-dioxaborolan-2-yl)phenyl)quinazolin-4(3*H*)-one (50 mg, 0.13 mmol), $Pd(Ph_3P)_4$ (5.8 mg, 5 μmol), and 2 M aqueous K_3PO_4 (0.15 mL, 0.3 mmol) in toluene (3 mL) and ethanol (1 mL) was heated at 110 °C for 9 h. The reaction mixture was diluted with ethyl acetate, the organics washed with

water and concentrated. The resulting residue was purified by chromatography (eluting with 90:9:1 DCM:MeOH:NH_4OH/97:2.7:0.3 DCM:MeOH:NH_4OH, 0-100% gradient) to give **17** (39 mg, 71%) as a white solid. LCMS *m/z* $(M+H)^+$ 521.3, $(M+H-H2O)^+$ 503.3. ^1H NMR (400 MHz, $CDCl_3$) δ 10.57 (d, *J*=15.18 Hz, 1H), 8.11 (d, *J*=6.38 Hz, 1H), 8.03 (ddd, *J*=8.42, 5.45, 3.08 Hz, 1H), 7.78-7.84 (m, 1H), 7.70 (d, *J*=1.76 Hz, 1H), 7.66 (dd, *J*=7.92, 3.74 Hz, 1H), 7.41-7.58 (m, 5H), 7.25 (br s, 1H), 7.12-7.16 (m,1H), 6.89-7.08 (m, 1H), 1.90 (d, *J*=12.10 Hz, 3H), 1.63-1.66 (m, 6H) (some exchangeable protons diffuse and not observed). ^1H NMR shows a mixture of atropisomers.

4-(3-(6-Fluoro-4-oxoquinazolin-3(4*H*)-yl)-2-methylphenyl)-7-(2-hydroxypropan-2-yl)-9*H*-carbazole-1-carboxamide (18).

Step A. 6-Fluoro-3-(2-methyl-3-(4,4,5,5-tetramethyl-1,3,2-dioxaborolan-2-yl)phenyl)quinazolin-4(3*H*)-one. The title compound was synthesized following the same procedures as described for the syntheses of **50** and **51** in 51% yield for the two steps (1.25 g). LCMS *m/z* 381.2 $(M+H)^+$. ^1H NMR (400MHz, $CDCl_3$) δ 8.00 (dd, *J*=8.4, 2.9 Hz, 1H), 7.94 (dd, *J*=7.5, 1.5 Hz, 1H), 7.92 (s, 1H), 7.80 (dd, *J*=9.0, 4.8 Hz, 1H), 7.57-7.50 (m, 1H), 7.38-7.32 (m, 1H), 7.32-7.28 (m, 1H), 2.35 (s, 3H), 1.35 (s, 12H).

Step B. 4-(3-(6-Fluoro-4-oxoquinazolin-3(4*H*)-yl)-2-methylphenyl)-7-(2-hydroxypropan-2-yl)-9*H*-carbazole-1-carboxamide (18). A mixture of **31** (35 mg, 0.1 mmol), 6-fluoro-3-(2-methyl-3-(4,4,5,5-tetramethyl-1,3,2-dioxaborolan-2-yl)phenyl)quinazolin-4(3*H*)-one (50 mg, 0.13 mmol), $Pd(Ph_3P)_4$ (6 mg, 5 μmol), and 2 M aqueous K_3PO_4 (0.15 mL, 0.3 mmol) in toluene (3 mL) and ethanol (1 mL) was heated at 110 °C for 8 h. The reaction mixture was diluted with ethyl acetate, washed with water and concentrated. The resulting residue was purified by chromatography (eluting with 90:9:1 DCM:MeOH:NH_4OH/97:2.7:0.3 DCM:MeOH:NH_4OH, 0-70% gradient) to give **18** (36 mg, 65%) as a white solid. LCMS *m/z* $(M+H)^+$ 521.3. ^1H NMR (400 MHz, $CDCl_3$) δ 10.57 (d, *J*=15.19 Hz, 1H), 8.11 (d, *J*=6.38 Hz, 1H), 8.03 (ddd, *J*=8.42, 5.45, 2.86 Hz, 1H), 7.78-7.84 (m, 1H), 7.70 (d, *J*=1.76 Hz, 1H), 7.66 (dd, *J*=7.70, 3.52 Hz, 1H), 7.40-7.59 (m, 5H), 7.14 (d, *J*=7.48 Hz, 1H), 6.86-7.08 (m, 1H), 1.90 (d,

J=12.10 Hz, 3H), 1.82 (d, *J*=13.42 Hz, 1H), 1.62 - 1.68 (m, 6H) (some exchangeable protons diffuse and not observed). ^{1}H NMR shows a mixture of atropisomers.

4-(3-(7-Fluoro-4-oxoquinazolin-3(4*H*)-yl)-2-methylphenyl)-7-(2-hydroxypropan-2-yl)-9*H*-carbazole-1-carboxamide (19).

Step A. 7-Fluoro-3-(2-methyl-3-(4,4,5,5-tetramethyl-1,3,2-dioxaborolan-2-yl)phenyl)quinazolin-4(3*H*)-one. The title compound was synthesized following the same procedures as described for the syntheses of **50** and **51** in 44% yield for the two steps (1.6 g). LCMS *m/z* 381.0 $(M+H)^+$.

Step B. 4-(3-(7-Fluoro-4-oxoquinazolin-3(4*H*)-yl)-2-methylphenyl)-7-(2-hydroxypropan-2-yl)-9*H*-carbazole-1-carboxamide (19). A mixture of **31** (35 mg, 0.1 mmol), 7-fluoro-3-(2-methyl-3-(4,4,5,5-tetramethyl-1,3,2-dioxaborolan-2-yl)phenyl)quinazolin-4(3*H*)-one (50 mg, 0.13 mmol), 2 M aqueous K_3PO_4 (0.15 mL, 0.3 mmol), and $Pd(Ph_3P)_4$ (6 mg, 5 μmol) in a mixture of toluene (3 mL) and ethanol (1 mL) was heated at 110 °C for 15 h. The mixture was cooled to RT, diluted with ethyl acetate and washed with water. The organics were concentrated and the residue was purified by chromatography (eluting with 90:9:1 DCM:MeOH:NH_4OH/97:2.7:0.3 DCM:MeOH:NH_4OH, 0-100% gradient) to give **19** (40 mg, 70%) as a white solid. LCMS *m/z* $(M+H)^+$ 521.1. ^{1}H NMR (400 MHz, $CDCl_3$) δ 10.57 (d, *J*=14.97 Hz, 1H), 8.41 (ddd, *J*=9.02, 5.94, 3.08 Hz, 1H), 8.15 (d, *J*=6.16 Hz, 1H), 7.68-7.71 (m, 1H), 7.65 (dd, *J*=7.70, 1.76 Hz, 1H), 7.41-7.56 (m, 4H), 7.22-7.31 (m, 2H), 6.87-7.16 (m, 2H), 5.90 (br s, 2H), 1.90 (d, *J*=11.66 Hz, 3H), 1.82 (d, *J*=12.10 Hz, 1H), 1.63-1.67 (m, 6H). ^{1}H NMR shows a mixture of atropisomers.

4-(3-(8-Fluoro-4-oxoquinazolin-3(4*H*)-yl)-2-methylphenyl)-7-(2-hydroxypropan-2-yl)-9*H*-carbazole-1-carboxamide (20).

Step A. 8-Fluoro-3-(2-methyl-3-(4,4,5,5-tetramethyl-1,3,2-dioxaborolan-2-yl)phenyl)quinazolin-4(3*H*)-one. The title compound was synthesized following the same procedures as described for the syntheses of **50** and **51** in 34% yield for the two steps (0.55 g). LCMS *m/z* 381.2 $(M+H)^+$. ^{1}H NMR (400 MHz, $CDCl_3$) δ 8.16 (d, *J*=7.5 Hz, 1H), 8.00 (s, 1H), 7.95 (d, *J*=7.3 Hz, 1H), 7.60-7.46 (m, 2H), 7.40-7.28 (m, 2H), 2.37 (s, 3H), 1.36 (s, 12H).

Step B. 4-(3-(8-Fluoro-4-oxoquinazolin-3(4*H*)-yl)-2-methylphenyl)-7-(2-hydroxypropan-2-yl)-9*H*-carbazole-1-carboxamide (20). A mixture of **31** (43 mg, 0.12 mmol), 8-fluoro-3-(2-methyl-3-(4,4,5,5-tetramethyl-1,3,2-dioxaborolan-2-yl)phenyl)quinazolin-4(3*H*)-one (61 mg, 0.16 mmol), $Pd(Ph_3P)_4$ (7 mg, 6 μmol), and 2 M aqueous K_3PO_4 (0.19 mL, 0.37 mmol) in a mixture of toluene (3 mL) and ethanol (1 mL) was heated at 110 °C overnight. The reaction mixture was diluted with ethyl acetate, washed with water and concentrated. The resulting residue was purified by chromatography (eluting with 90:9:1 DCM:MeOH:NH_4OH/97:2.7:0.3 DCM:MeOH:NH_4OH, 0-100% gradient) to give **20** (50 mg, 71%) as a white solid. LCMS *m/z* $(M+H)^+$ 521.3. ^1H NMR (400 MHz, $CDCl_3$) δ 10.59 (m, 1H), 8.18 (d, *J*=7.26 Hz, 2H), 7.71 (dd, *J*=10.01, 0.99 Hz, 1H), 7.65 (t, *J*=7.70 Hz, 1H), 7.41-7.59 (m, 5H), 7.20-7.29 (m, 1H), 7.07 (dd, *J*=17.83, 7.70 Hz, 1H), 6.87-7.15 (m, 1H), 2.00 (d, *J*=14.97 Hz, 1H), 1.89 (d, *J*=12.54 Hz, 3H), 1.64 (s, 6H) (some exchangeable protons diffuse and not observed). ^1H NMR shows a mixture of atropisomers.

7-(Hydroxymethyl)-4-(2-methyl-3-(4-oxoquinazolin-3(4*H*)-yl)phenyl)-9*H*-carbazole-1-carboxamide (21).

Step A. 4-Bromo-7-(hydroxymethyl)-9*H*-carbazole-1-carboxamide (32). To a cloudy solution of **30** (0.5g, 1.38 mmol) in THF (28 mL) at 0°C was added lithium aluminum hydride (3.46 mL, 3.46 mmol, 1M in THF). The reaction was brought to RT, stirred for 2 h and quenched with water. The reaction mixture was brought to pH ~8-9 with the addition of 1N HCl, then partitioned between EtOAc and water. The organic phase was washed with sat. $NaHCO_3$, brine, dried over Na_2SO_4, and concentrated to afford **32** (0.37 g, 84%) as a light pink solid. LCMS *m/z* 318.9, 320.9 $(M+H)^+$. ^1H NMR (400 MHz, DMSO-d_6) δ 11.67 (s, 1H), 8.52 (d, *J*=8.3 Hz, 1H), 8.20 (br s, 1H), 7.82 (d, *J*=8.3 Hz, 1H), 7.77 (s, 1H), 7.56 (br s, 1H), 7.41 (d, *J*=8.3 Hz, 1H), 7.22 (d, *J*=8.3 Hz, 1H), 5.29 (t, *J*=5.7 Hz, 1H), 4.66 (d, *J*=5.7 Hz, 2H).

Step B. 7-(Hydroxymethyl)-4-(2-methyl-3-(4-oxoquinazolin-3(4*H*)-yl)phenyl)-9*H*-carbazole-1-carboxamide (21). A mixture of **32** (40 mg, 0.12 mmol), **51** (45 mg, 0.12 mmol), $Pd(Ph_3P)_4$ (7 mg, 6.3 umol) and 2 M aqueous K_3PO_4 (0.16 mL, 0.3 mmol) in THF (2 mL) was degassed with nitrogen and

heated at 90 °C for 16 h. The reaction mixture was diluted with DCM, washed with saturated $NaHCO_3$ and concentrated. The resulting residue was purified by chromatography (eluting with 0-100% ethyl acetate/hexane) to give **21** (22 mg, 36%) as a light yellow solid. LCMS *m/z* 474.9 $(M+H)^+$. ^1H NMR (400 MHz, CD_3OD) δ 8.29-8.39 (m, 2H), 7.95 (dd, *J*=7.81, 6.05 Hz, 1H), 7.85-7.92 (m, 1H), 7.76 - 7.82 (m, 1H), 7.48-7.65 (m, 5H), 7.23 (d, *J*=8.14 Hz, 1H), 7.06-7.13 (m, 1H), 6.98-7.06 (m, 1H), 4.70-4.76 (m, 2H), 1.82 (s, 3H). ^1H NMR shows a mixture of atropisomers.

7-(2-Hydroxypropan-2-yl)-4-(3-(4-oxoquinazolin-3(4*H*)-yl)phenyl)-9*H*-carbazole-1-carboxamide (22).

Step A. 3-(3-(4,4,5,5-Tetramethyl-1,3,2-dioxaborolan-2-yl)phenyl)quinazolin-4(3*H*)-one. The title compound was synthesized following the same procedures as described for the syntheses of **50** and **51** in 34% yield for the two steps (0.8 g). LCMS *m/z* $(M+H)^+$ 349.1. ^1H NMR (400 MHz, $CDCl_3$) δ 8.37 (dd, *J*=8.0, 1.0 Hz, 1H), 8.13 (s, 1H), 7.94-7.90 (m, 1H), 7.86-7.75 (m, 3H), 7.58-7.50 (m, 3H), 1.35 (s, 11H).

Step B. 7-(2-Hydroxypropan-2-yl)-4-(3-(4-oxoquinazolin-3(4*H*)-yl)phenyl)-9H-carbazole-1-carboxamide (22). A mixture of **31** (40 mg, 0.12 mmol), 3-(3-(4,4,5,5-tetramethyl-1,3,2-dioxaborolan-2-yl)phenyl)quinazolin-4(3*H*)-one (52 mg, 0.15 mmol), 2 M aqueous K_3PO_4 (0.17 mL, 0.35 mmol), and $Pd(Ph_3P)_4$ (6.7 mg, 5.8 μmol) in a mixture of toluene (3 mL) and ethanol (1 mL) was heated at 110 °C for 8 h. The reaction mixture was diluted with ethyl acetate and the organics washed with water then concentrated. The resulting yellow residue was purified by chromatography (eluting with 90:9:1 DCM:MeOH:NH_4OH/97:2.7:0.3 DCM:MeOH:NH_4OH, 0-100% gradient) to give **22** (48 mg, 81%) as a white solid. LCMS *m/z* $(M+H-H2O)^+$ 471.0, $(M+H)^+$ 489.1. ^1H NMR (400 MHz, $CDCl_3$) δ 10.62 (s, 1H), 8.40 (dd, *J*=8.03, 0.77 Hz, 1H), 8.24 (s, 1H), 7.71-7.84 (m, 4H), 7.69 (d, *J*=1.54 Hz, 2H), 7.54-7.64 (m, 4H), 7.20 (dd, *J*=8.47, 1.65 Hz, 1H), 7.13 (d, *J*=7.92 Hz, 1H), 6.00 (br s, 2H), 1.87 (s, 1H), 1.65 (s, 6H).

4-(2-Fluoro-3-(4-oxoquinazolin-3(4*H*)-yl)phenyl)-7-(2-hydroxypropan-2-yl)-9*H*-carbazole-1-carboxamide (23).

Step A. 3-(3-Bromo-2-fluorophenyl)quinazolin-4(3*H*)-one. A mixture of 3-bromo-2-fluoroaniline (1 g, 5.3 mmol), 2-aminobenzoic acid (866 mg, 6.3 mmol) and triethoxymethane (1.5 mL, 9 mmol) in toluene (25 mL) was heated to 110 °C for 20 h. The reaction mixture was then cooled to RT and concentrated. The resulting residue was dissolved in EtOAc, washed with 1M HCl, sat. $NaHCO_3$, and brine. The organic layer was then dried over Na_2SO_4, filtered and concentrated. The crude residue was purified by chromatography (eluting with EtOAc/hexane, 0-50% gradient) to give 3-(3-bromo-2-fluorophenyl)quinazolin-4(3*H*)-one (675 mg, 38%) as an off-white solid. LCMS *m/z* $(M + H)^+$ 318.9. ^{1}H NMR NMR (400 MHz, DMSO-d6) δ 8.41 (s, 1H), 8.22 (dd, *J*=8.1, 1.3 Hz, 1H), 7.96–7.88 (m, 2H), 7.78 (d, *J*=8.1 Hz, 1H), 7.76–7.70 (m, 1H), 7.64 (t, *J*=7.6 Hz, 1H), 7.39 (td, *J*=8.1, 1.0 Hz, 1H).

Step B. 4-(2-Fluoro-3-(4-oxoquinazolin-3(4*H*)-yl)phenyl)-7-(2-hydroxypropan-2-yl)-9*H*-carbazole-1-carboxamide (23). A mixture of **33** (297 mg, 0.75 mmol), 3-(3-bromo-2-fluorophenyl)quinazolin-4(3*H*)-one (200 mg, 0.63 mmol), and 2 M aqueous Na_2CO_3 (1.097 mL, 2.193 mmol) in toluene (7 mL) and ethanol (7 mL) was sonicated and degassed with nitrogen for 5 min. To this mixture was added $Pd(Ph_3P)_4$ (36 mg, 0.031 mmol) and the reaction was heated to 85 ^{o}C for 18 h. The reaction mixture was then concentrated and brine and EtOAc were added. The organic phase was extracted, dried over Na_2SO_4, filtered and concentrated. The resulting dark solid was purified by chromatography (eluting with MeOH/DCM, 0-10% gradient) to afford **23**, which was further purified by preparative HPLC (Phenomenex Luna Axia, 5µ, 30x100 mm, solvent A: 10% CH_3CN- 90% H_2O- 0.1% TFA; solvent B: 90% CH_3CN - 10% H_2O- 0.1% TFA, gradient: 30-100% B, gradient time: 10 min, flow rate: 30 ml/min, wavelength 254 nm) to give **23** (209 mg, 65%) as an off-white solid. LCMS (EI) *m/z* (M + H)+ 507.1. ^{1}H-NMR (400 MHz, DMSO-d6) δ 11.47 (s, 1H), 8.54 (br s, 1H), 8.27–8.14 (m, 2H), 8.00 (d, *J*=7.7 Hz, 1H), 7.96–7.84 (m, 3H), 7.81–7.71 (m, 2H), 7.66–7.58 (m, 2H), 7.51 (br s, 1H), 7.31 (br s, 1H), 7.19–7.08 (m, 2H), 5.00 (s, 1H), 1.47 (s, 6H).

Human recombinant BTK enzyme assay: To V-bottom 384-well plates were added test compounds, human recombinant BTK (1 nM, Invitrogen Corporation), fluoresceinated peptide (1.5

μM), ATP (20 μM (Km^{app})), and assay buffer (20 mM HEPES pH 7.4, 10 mM $MgCl_2$, 0.015% Brij 35 surfactant and 4 mM DTT in 1.6% DMSO), with a final volume of 30 μL. After incubating at room temperature for 60 min, the reaction was terminated by adding 45 μL of 35 mM EDTA to each sample. The reaction mixture was analyzed on the Caliper LabChip 3000 (Caliper, Hopkinton, MA) by electrophoretic separation of the fluorescent substrate and phosphorylated product (Excitation: 488nm, Emission: 530nm). Inhibition data were calculated by comparison to control reactions with no enzyme (for 100% inhibition) and controls with no inhibitor (for 0% inhibition). Dose response curves were generated to determine the concentration required for inhibiting 50% of BTK activity (IC_{50}). Compounds were dissolved at 10 mM in DMSO and evaluated at eleven concentrations.

Human recombinant LCK enzyme assay: Recombinant GST-LCK (PSS) was combined with a fluorescent substrate FITC-AHA-EGIYLFKKK-NH_2, ATP, and varying concentrations of inhibitors in a 384 well plate (Thermo Scientific). The final reaction volume (0.030 ml) contained 100 mM HEPES pH 7.4, 10 mM $MgCl_2$, 0.015% Brij-35, 0.4 mM DTT, 6 μM ATP (Km^{app}), 3 μM FITC-AHA-EGIYLFKKK-NH_2, 0.5 nM GST-LCK, 1.6% DMSO, and varying concentrations of inhibitors (from 2 μM to 33 pM). Compound stock solutions (10 mM) were prepared in dimethyl sulfoxide (DMSO). Kinase reactions were incubated at room temperature for 1 hour and terminated by adding 60 μl of 35 mM EDTA buffer to each sample. Reaction solutions were analyzed on the Caliper LabChip 3000 (Caliper, Hopkinton, MA) by electrophoretic separation of the fluorescent substrate and phosphorylated product (Excitation: 488nm, Emission: 530nm). IC_{50} values were derived by non-linear regression analysis of the concentration response data.

BCR-Stimulated calcium flux in Ramos B cells: Human Ramos (RA1) B cells (ATCC CRL-1596) at a density of 2 x 106 cells/mL in RPMI minus phenol red (Invitrogen 11835-030) and 50 mM HEPES (Invitrogen 15630-130) containing 0.1% BSA (Sigma A8577) were added to one half volume of calcium loading buffer (BD bulk kit for probenecid sensitive assays, # 640177) and incubated at room temperature in the dark for 1 hour. Dye-loaded cells were pelleted (Beckmann GS-CKR, 1200 rpm, room temperature, 5 min) and resuspended at room temperature in RPMI minus phenol red with 50 mM

HEPES and 10% FBS to a density of 1 x 106 cells/mL. 150 µL aliquots (150,000 cells/well) were plated into 96 well poly-D-lysine coated assay plates (BD 35 4640) and briefly centrifuged (Beckmann GS-CKR 800 rpm, 5 min, without brake). Next, 50 µL compound dilutions in 0.4% DMSO/RPMI minus phenol red + 50 mM HEPES + 10% FBS were added to the wells and the plate was incubated at room temperature in the dark for 1 hour. The assay plate was briefly centrifuged as above prior to measuring calcium levels. Using the FLIPR1 (Molecular Devices), cells were stimulated by adding goat anti-human IgM (Invitrogen AHI0601) to 2.5 µg/mL. Changes in intracellular calcium concentrations were measured for 180 seconds and percent inhibition was determined relative to peak calcium levels seen in the presence of stimulation only.

Immune complex-stimulated TNFα production in peripheral blood mononuclear cells (PBMCs): Human peripheral blood mononuclear cells in media containing 10% FBS and various concentrations of test compound were stimulated for 7 h at 37 ^{o}C with immune complexes prepared from goat anti-human IgG (Jackson ImmunoResearch, cat# 109-005-003) and human IgG (Jackson ImmunoResearch, cat# 009-000-003), both of which were purified to remove endotoxin prior to immune complex generation. TNFα levels were measured by ELISA (TNF-alpha OptEIA BD Biosciences, cat# 5551212).

Whole blood assays of BCR-stimulated CD69 expression on B cells: To measure BCR-stimulated B cells, heparinized human whole blood was added with various concentrations of test compound and stimulated with 30 µg/mL AffiniPure F(ab')2 fragment goat anti human IgM (Jackson 109-006-1299 – endotoxin cleared) and 10 ng/mL human IL-4 (Peprotech 200-04) for 18 h at 37 ^{o}C with agitation. The cells were stained with FITC-conjugated mouse anti-human CD20 (BD Pharmingen 555622) and PE-conjugated mouse anti-human CD69 monoclonal antibody (BD Pharmingen 555531), lysed and fixed, then washed. The amount of CD69 expression was quantitated by the mean fluorescence intensity (MFI) after gating on the CD20-positive B cell population as measured by FACS analysis. B cells in mouse whole blood were stimulated in an similar way, using AffinPure F(ab')2 Fragment goat anti mouse IgG + IgM (Jackson Cat#115-006-068) at 100 µg/mL to stimulate, and

staining with allophycocyanin (APC) rat anti-mouse CD19 antibody (BD Biosciences 550992) to identify the B cells and CD69 quantitation with FITC-conjugated anti-mouse CD69 monoclonal antibody (BD Biosciences 553236).

In vivo studies

All animal procedures were conducted with the approval of the Bristol-Myers Squibb Animal Care and Use Committee and Committee for the Purpose of Control and Supervision of Experiments on Animals (CPCSEA; registration number 1089/RO/bc/2007/CPCSEA). Mice (Harlan Laboratories, Indianapolis, IN, USA and The Netherlands) were housed under a 12-hour/12-hour light/dark cycle and provided customary access to fresh drinking water and rodent chow diet ad libitum.

Pharmacokinetic (PK) analysis

Unless noted otherwise, in the in vivo studies described below, compound **6** was administered in a polyethylene glycol 400 (PEG-400)/water/ethanol (70:20:10, v/v/v) solution.

Single-dose PK in mice. Two groups of animals (N = 9 per group, 19-26 g) were fasted overnight and received compound **6** either as an intravenous (IV) bolus dose (2 mg/kg) via the tail vein or by oral gavage (5 mg/kg). Blood samples (~0.2 mL) were obtained by retro-orbital bleeding at 0.05 (or 0.25 for oral), 0.5, 1, 3, 6, 8, and 24 hours post dose. For IV dosing, mice were divided into three groups, one group was bled at 0.05, 0.5, and 6 hours and the second group was bled at 0.25, 3, and 8 hours, while the third group was bled at 1 and 24 h. For PO dosing, mice were also divided into three groups, one group was bled at 0.25, 1, and 6 hours, and the second group was bled at 0.5, 3, and 8 hours, while the third group was bled at 24 h; resulting in a composite PK profiles (3 mice per time point). Blood samples were allowed to coagulate and centrifuged at 4°C (1500-2000 x g) to obtain serum. Serum samples were stored at -20°C until analysis by LC/MS/MS.

Single-dose PK in rats. Male Sprague-Dawley rats (255-298 g) were used in the PK studies of **6**. IV doses were administered to non-fasted rats; oral doses were administered to fasted rats, which were allowed food 4 h post dose. Blood samples (~0.3 mL) were collected from the jugular vein into K_3EDTA-containing tubes and then centrifuged at 4°C (1500-2000 x g) to obtain plasma, which was stored at -20°C until analysis by LC/MS/MS.

To investigate the oral bioavailability of compound **6** after crystalline microsuspension doses, rats (N =) received the compound by oral gavage (1, 5, and 20 mg/kg). T99.5% 10 mM citrate buffer pH4, 0.02% DOSS, methocel A4M. Serial blood samples were obtained after oral dosing at 0.25, 0.5, 0.75, 1, 2, 4, 6, 8, and 24 hours post dose. Plasma samples, obtained by centrifugation at 4°C (1500-2000g), were stored at -20°C until analysis.

Single-dose PK in dogs. The PK of compound **6** was evaluated in male beagle dogs following IV infusion (2 mg/kg over 10 minutes) via a femoral vein or by oral administration (2 mg/kg) (kg). The studies were conducted in a crossover design (N = 3), with one week washout period between the IV and oral studies. IV doses were administered to nonfasted dogs; oral doses were administered to fasted dogs, which were allowed food 4 h post dose. Serial blood samples were collected at 0.167 (IV only), 0.25, 0.5, 0.75, 1, 2, 4, 6, 8, 10, 12, 24 and 48 hours post-dose, followed by centrifugation at 4°C (1500-2000g) to obtain plasma. All samples were stored at -20°C until analysis by LC/MS/MS.

Single-dose PK in monkeys. Compound **6** was evaluated in male cynomolgus monkeys, following IV infusion (2 mg/kg over 10 minutes) via a femoral vein port or by oral administration (2 mg/kg) (4.6 to 6.2 kg). The studies were conducted in a crossover design (N = 3), with one week washout period between the IV and oral studies. IV doses were administered to nonfasted monkeys; oral doses were administered to fasted monkeys, which were allowed food 4 h post dose. Serial blood samples were collected at 0.167 (IV only), 0.25, 0.5, 0.75, 1, 2, 4, 6, 8, 10, 12, 24 and 48 hours post-dose, followed by

centrifugation at 4°C (1500-2000g) to obtain plasma. All samples were stored at -20°C until analysis by LC/MS/MS.

Primary anti-KLH antibody responses in mice: Female BALB/c mice (8-12 weeks old, Harlan) were immunized intraperitoneally (IP) with 250 μg KLH (Pierce, Rockford, IL) in PBS on Day 0. Mice in appropriate groups were dosed daily by oral gavage with vehicle (EtOH:TPGS:PEG300; 5:5:90) or test compound. Blood was collected on Days 7 and 14 post-immunization. Serum was separated and analyzed for anti-KLH IgM titers (Day 7) and anti-KLH IgG titers (Day 14) by ELISA. Briefly, 96 well plates were coated with KLH in PBS, blocked, and serial dilutions of test serum samples were added. Captured anti-KLH antibodies were detected using horseradish peroxidase-conjugated antibody specific for mouse IgM or IgG (Southern Biotechnology Associates, Birmingham, AL) and the TMB peroxidase substrate system (Kirkegaard and Perry Laboratories, Gaithersburg, MD). Optical densities of developed plates were quantitated in a SpectraMax Plus ELISA plate reader (Molecular Devices, Sunnyvale, CA). Serum from BALB/c mice collected on Day 7 (IgM) or on Day 14 (IgG) after immunization with KLH was pooled and used as a standard comparator in each respective assay. The data are expressed by relating the test sample titers to the standard comparator titer which was assigned a value of 1.

Collagen-induced arthritis in mice: DBA/1 male mice (8-10wk of age; Harlan) were immunized subcutaneously at the base of the tail on Day 0 and again on Day 21 with 200 μg bovine type II collagen admixed with reconstituted Sigma Adjuvant System (SAS; Sigma-Aldrich). For "preventative" dosing, mice were dosed daily (beginning on Day 0) by oral gavage with vehicle (EtOH:TPGS:PEG300; 5:5:90) or compound **6**. For "pseudo-established" dosing, the start of dosing was delayed until the Day 21 booster immunization. Following the booster immunization, mice were monitored 3 times per week for the development and severity of paw inflammation. Each paw was visually scored by the following scheme: +0 = normal. +1 = one (or more) joints inflamed on digits. +2 = mild-moderate inflammation of plantar surface of paw and paw thickness modestly increased. +3 = moderate-severe inflammation of

plantar surface of paw and paw thickness significantly increased. +4 = ankylosis of ankle joint (significantly reduced hock joint motion on flexion/extension). Unblinded clinical paw scores for all four paws were summed for each mouse, and mean ± SEM was calculated for each treatment group.

For histological evaluation, rear paws were fixed, decalcified and embedded in paraffin. Sections were cut in the sagittal plane, stained in H & E and evaluated microscopically without knowledge of treatment group. Lesions were scored on a severity scale of 0 (normal) to 4 in two separate categories, inflammation (cellular infiltration and pannus formation) and bone resorption. Bone morphology and bone mineral density of hind paws excised postmortem was analyzed by micro-computed tomography (micro-CT) after fixation in 10% Neutral Buffered Formalin. Age-matched naïve (disease-free) paws were used as a control for comparative micro-CT analysis. The analysis was conducted in a blinded format.

Micro-computed tomography imaging and histopathology: Bone morphology was evaluated by micro-CT using the Scanco VivaCT40 (Scanco Medical AG, Zurich, Switzerland). Imaging parameters included approximately 500 slices (21-μm thick) acquired with 250 projections, 500-ms integration time, 55 kVp photon energy, and 145 μA of current. Region of interest (ROI) focused on the hind/mid foot sections (talus to proximal end of the first metatarsal bone). Threshold settings were optimized using histomorphometric methods. Bone mineral density (BMD) and bone surface area (BSA) were evaluated using a hydroxylapatite calibration phantom and Scanco proprietary software. The analysis was conducted in a blinded format.

Collagen antibody-induced arthritis in mice: Female BALB/c mice (8-10 weeks of age; Harlan) were injected IP with a mixture of four monoclonal anti-mouse type II collagen antibodies (1 mg of each). Daily oral dosing was immediately started with vehicle (EtOH:TPGS:PEG300; 5:5:90), compound **6** (10 or 30 mg/kg) or dexamethasone (1 mg/kg). Three days later, the mice were injected IP with 1.25 mg/kg LPS (E. coli O111:B4; Sigma). Thereafter, mice were monitored 3X/wk for the development and severity of paw inflammation. Each paw was visually scored by the following scheme: +0 = normal. +1 = one (or more) joints inflamed on digits. +2 = mild-moderate inflammation

of plantar surface of paw and paw thickness modestly increased. +3 = moderate-severe inflammation of plantar surface of paw and paw thickness significantly increased. +4 = ankylosis of ankle joint (significantly reduced hock joint motion on flexion/extension). Unblinded clinical paw scores for all four paws were summed for each mouse, and mean ± SEM was calculated for each treatment group.

X-ray crystallography: A baculovirus construct of His-TEV-hBTK (E396-S659) was used to generate protein for X-ray crystallography as previously reported.[24] For protein/compound complex formation, 4 μL of compound **23** (50 mM DMSO stock) was added to 1.5 mL of hBTK at 0.35 mg/mL and incubated at room temperature for 3 h and then concentrated to 5.25 mg/mL prior to set up drops. Crystals were grown at room temperature using hanging drop vapor diffusion method. The drop consisted of 3 μL protein solution and 1 μL reservoir solution containing 31% (w/v) methyl ether PEG 5000, 1% (w/v) PEG 8000, 0.2 M Tris-HCl, pH 8.5. Macroseeding was performed to initiate crystal growth. The crystals appeared within a few days and continued to grow for 2-3 weeks. Crystals were flash-cooled in liquid nitrogen for data collection with 25% glycerol and 75% reservoir solution as cryoprotectant. Diffraction data were collected by Shamrock Structures, Inc. at IMCA-CAT, beamline 17ID at the Advanced Photon Source. hBTK/compound **23** co-crystals belonged to the space group $p2_1$: a=63.5Å, b=45.5Å, c=98.4Å, α=λ=90.0°, β=94.0°. The 1.97Å resolution structure was determined by molecular replacement using a previously determined in house BTK structure (unpublished results). The structure of hBTK + compound **23** has been deposited to RCSB with PDB ID 5JRS.

ANCILLARY INFORMATION

Supporting Information

PDB ID Codes: 5JRS for compound 23. Authors will release the atomic coordinates and experimental data upon article publication.

Molecular formula strings and the associated biological data (CSV).

The Supporting Information is available free of charge on the ACS Publications website at HTTP://PUBS.ACS.ORG.

AUTHOR INFORMATION

Corresponding Authors

*E-mail: joseph.tino@bms.com Phone: 609-252-4809. Fax: 609-252-7410.

*E-mail: george.delucca@bms.com. Phone: 609-252-3121.

Notes

The authors declare no competing financial interest.

ABBREVIATIONS USED

BTK, Bruton's Tyrosine Kinase; LCK, lymphocyte-specific protein tyrosine kinase; SFC, super critical fluid chromatography; hERG, human ether-a-go-go-related gene; WB, whole blood; PBMC, human peripheral blood mononuclear cells; APC, antigen presenting cell; SLE, systemic lupus erythematosus; RA, rheumatoid arthritis; DOSS, dioctyl sodium sulfosuccinate; BCS, Biopharmaceutics Classification System;

References

(1) (a) Volkamer, A.; Eid, S.; Turk, S.; Jaeger, S.; Rippmann, F.; Fulle, S. Pocketome of human kinases: Prioritizing the ATP binding sites of (yet) untapped protein kinases for drug discovery. *J. Chem. Inform. Mod*. **2015**, *55*, 282-293. (b) Gross, S.; Rahal, R.; Stransky, N.; Lengauer, C.; Hoeflich, K. P. Targeting cancer with kinase inhibitors. *J. Clin. Invest.* **2015**, *125*, 1780-1789. (c) Daub, H. Quantitative proteomics of kinase inhibitor targets and mechanisms. *ACS Chem. Biol.* **2015**, *10*, 201-212.

(2) (a) Mohamed, A. J.; Yu, L.; Bäckesjö, C.-M.; Vargas, L.; Faryal, R.; Aints, A.; Christensson, B.; Berglöf, A.; Vihinen, M.; Nore, B. F.; Smith, C. I. E. Bruton's tyrosine kinase (Btk): function, regulation, and transformation with special emphasis on the PH domain. *Immunol. Rev.* **2009**, 228, 58-73; b) Mohamed, A. J.; Nore, B. F.; Christensson, B.; Smith, C. I. E. Signaling of Bruton's tyrosine kinase, Btk. *Scand. J. Immunol.* **1999**, *49*, 113-118.

(3) (a) Jongstra-Bilen, J.; Puig Cano, A.; Hasija, M.; Xiao, H.; Smith, C. I.; Cybulsky, M. I. Dual functions of Bruton's tyrosine kinase and Tec kinase during Fcγ receptor-induced signaling and phagocytosis. *J. Immunol.* **2008**, *181*, 288-298. (b) Kuehn, H. S.; Radinger, M.; Brown, J. M.; Ali, K.; Vanhaesebroeck, B.; Beaven, M. A.; Metcalfe, D. D.; Gilfillan, A. M.. Btk-dependent Rac activation and actin rearrangement following FcεRI aggregation promotes enhanced chemotactic responses of mast cells. *J. Cell Sci.* **2010**, *123*, 2576-2585. c) Tsukada, S.; Rawlings, D. J.; Witte, O. N. Role of Bruton's tyrosine kinase in immunodeficiency. *Curr. Opin. Immunol.* **1994**, *6*, 623-630.

(4) Lee, S. H.; Kim, T.; Jeong, D.; Kim, N.; Choi, Y. The Tec family tyrosine kinase Btk regulates RANKL-induced osteoclast maturation. *J. Biol. Chem*. **2008**, *283*, 11526-11534.

(5) Mease, P. J. B cell-targeted therapy in autoimmune disease: rationale, mechanisms, and clinical application. *J. Rheumatol.* **2008**, *35*, 1245-1255.

(6) Goldstein, M. D.; Debenedette, M. A.; Hollenbaugh, D.; Watts, T. H. Induction of costimulatory molecules B7-1 and B7-2 in murine B cells: the CBA/N mouse reveals a role for Bruton's tyrosine kinase in CD40-mediated B7 induction. *Molec. Immunol.* **1996**, *33*, 541-552.

(7) (a) Jansson, L.; Holmdahl, R. Genes on the X chromosome affect development of collagen-induced arthritis in mice. *Clin. Exp. Immunol*. **1993**, *94*, 459-465. (b) Steinberg, B. J.; Smathers, P. A.; Frederiksen, K.; Steinberg, A. D. Ability of the XID gene to prevent autoimmunity in

(NZBXNZW)F1 mice during the course of their natural history, after polyclonal stimulation, or following immunization with DNA. *J. Clin. Invest.* **1982**, *70*, 587-597.

(8) (a) Xu, D.; Kim, Y.; Postelnek, J.; Vu, M. D; Hu, D.-Q.; Liao, C.; Bradshaw, M.; Hsu, J.; Zhang, J.; Pashine, A.; Srinivassan, D.; Woods, J.; Levin, A.; O'Mahony, A.; Owens, T. D.; Lou, Y.; Hill, R. J.; Narula, S.; DeMartino, J.; Fine, J. S. RN486, a selective Bruton's tyrosine kinase inhibitor, abrogates immune hypersensitivity responses and arthritis in rodents. *J. Pharmacol. Exp. Ther.* **2012**, *341*, 90-103. (b) Rankin, A. L.; Seth, N.; Keegan, S.; Andreyeva, T.; Cook, T. A.; Edmonds, J.; Mathialagan, N.; Benson, M. J.; Syed, J.; Zhan, Y.; Benoit, S. E.; Miyashiro, J. S.; Wood, N.; Mohan, S.; Peeva, E.; Ramaiah, S. K.; Messing, D.; Homer, B. L.; Dunussi-Joannopoulos, K.; Nickerson-Nutter, C. L.; Schnute, M. E.; Douhan, J., III. Selective inhibition of BTK prevents murine lupus and antibody-mediated glomerulonephritis. *J. Immunol*. **2013**, *193*, 4540-4550.

(9) (a) Puck, J. M. Molecular and genetic basis of X-linked immunodeficiency disorders. *J. Clin. Immunol*. **1994**, *14*, 81-89. (b) Hendriks, R. W.; Bredius, R. G. M.; Pike-Overzet, K.; Staal, F. J. T. Biology and novel treatment options for XLA, the most common monogenetic immunodeficiency in man. *Expert Opin. Ther. Targets* **2011**, *15*, 1003-1021. (c) Lederman, H. M.; Winkelstein, J. A. X-linked agammaglobulinemia: an analysis of 96 patients. *Medicine* **1985**, *64*, 145-156.

(10) (a) Cohen, M. S.; Zhang, C.; Shokat, K. M.; Taunton, J. Structural bioinformatics-based design of selective, irreversible kinase inhibitors. *Science* **2005**, *308*, 1318-1321. (b) Leproult, E.; Barluenga, S.; Moras, D.; Wurtz, J. M.; Winssinger, N. Cysteine mapping in conformationally distinct kinase nucleotide binding sites: application to the design of selective covalent inhibitors. *J. Med. Chem*. **2011**, *54*, 1347-1355.

(11) Honigberg, L. A.; Smith, A. M.; Sirisawad, M.; Verner, E.; Loury, D.; Chang, B.; Li, S.; Pan, Z.; Thamm, D. H.; Miller, R. A.; Buggy, J. J. The Bruton tyrosine kinase inhibitor PCI-32765 blocks B-cell activation and is efficacious in models of autoimmune disease and B-cell malignancy. *Proc. Natl. Acad. Sci.* **2010**, *107*, 13075-13080.

(12) (a) Burger, J. A. Bruton's Tyrosine Kinase (BTK) Inhibitors in Clinical Trials. *Curr. Hematol. Malig. Rep*. **2014**, *9*, 44-49. (b) Akinleye, A.; Chen, Y.; Mukhi, N.; Song, Y.; Liu, D. Ibrutinib and novel BTK inhibitors in clinical development. *J. Hematol. Oncol*. **2013**, *6*, 59-67. (c) Whang, J. A.; Chang, B. Y. Bruton's tyrosine kinase inhibitors for the treatment of rheumatoid arthritis. *Drug Disc. Today* **2014**, *19*, 1200-1204.

(13) (a) Park, J. K.; Park, J. A.; Lee, Y. J.; Song, J.; Oh, J. I.; Lee, Y.-M.; Suh, K. H.; Son, J.; Lee, E. B. HM71224, a novel oral BTK inhibitor, inhibits human immune cell activation: New drug candidate to treat B-cell associated autoimmune diseases. *Ann. Rheum. Dis.* **2014**, *73*, 355-356. (b) Bradshaw, J. M.; McFarland, J. M.; Paavilainen, V. O.; Bisconte, A.; Tam, D.; Phan, V. T.; Romanov, S.; Finkle, D.; Shu, J.; Patel, V.; Ton, T.; Li, X.; Loughhead, D. G.; Nunn, P. A.; Karr, D. E.; Gerritsen, M. E.; Funk, J. O.; Owens, T. D.; Verner, E.; Brameld, K. A.; Hill, R. J.; Goldstein, D. M.; Taunton, J. Prolonged and tunable residence time using reversible covalent kinase inhibitors. *Nat. Chem. Bio*. **2015**, *11*, 525-531.

(14) Evans, E. K.; Tester, R.; Aslanian, S.; Karp, R.; Sheets, M.; Labenski, M. T.; Witowski, S. R.; Lounsbury, H.; Chaturvedi, P.; Mazdiyasni, H.; Zhu, Z.; Nacht, M.; Freed, M. I.; Petter, R. C.; Dubrovskiy, A.; Singh, J.; Westlin, W. F. Inhibition of Btk with CC-292 provides early pharmacodynamic assessment of activity in mice and humans. *J. Pharmacol. Exp. Ther*. **2013**, *346*, 219-228.

(15) (a) Young, W. B.; Barbosa, J.; Blomgren, P.; Bremer, M. C.; Crawford, J. J.; Dambach, D.; Gallion, S.; Hymowitz, S. G.; Kropf, J. E.; Lee, S. H.; Liu, L.; Lubach, J. W.; Macaluso, J.;

Maciejewski, P.; Maurer, B.; Mitchell, S. A.; Ortwine, D. F.; Di Paolo, J.; Reif, K.; Scheerens, H.; Schmitt, A.; Sowell, C. G.; Wang, X.; Wong, H.; Xiong, J.-M.; Xu, J.; Zhao, Z.; Currie, K. S. Potent and selective Bruton's tyrosine kinase inhibitors: discovery of GDC-0834. *Bio. Med. Chem. Lett.* **2015**, *25*, 1333-1337. (b) Young, W. B.; Barbosa, J.; Blomgren, P.; Bremer, M. C.; Crawford, J. J.; Dambach, D.; Eigenbrot, C.; Gallion, S.; Johnson, A. R.; Kropf, J. E.; Lee, S. H.; Liu, L.; Lubach, J. W.; Macaluso, J.; Maciejewski, P.; Mitchell, S. A.; Ortwine, D. F.; Di Paolo, J.; Reif, K.; Scheerens, H.; Schmitt, A.; Wang, X.; Wong, H.; Xiong, J.-M.; Xu, J.; Yu, C.; Zhao, Z.; Currie, K. S. Discovery of highly potent and selective Bruton's tyrosine kinase inhibitors: pyridazinone analogs with improved metabolic stability. *Bio. Med. Chem. Lett.* **2016**, *26*, 575-579.

(16) Liu, J.; Guiadeen, D.; Krikorian, A.; Gao, X.; Wang, J.; Boga, S. B.; Alhassan, A.-B.; Yu, Y.; Vaccaro, H.; Liu, S.; Yang, C.; Wu, H.; Cooper, A.; De Man, A.; Kaptein, A.; Maloney, K.; Horvak, V.; Gao, Y.-D.; Fischmann, T. O.; Raaijmakers, H.; Vu-Pham, D.; Presland, J.; Manusueto, M.; Xu, Z.; Leccese, E.; Zhang-Hoover, J.; Knemeyer, I.; Garlisi, C. G.; Bays, N.; Stivers, P.; Brandish, P. E.; Hicks, A.; Kim, R.; Kozlowski, J. A. Discovery of 8-amino-imidazo[1,5-a]pyrazines as reversible selective BTK inhibitors for the treatment of rheumatoid arthritis. *ACS Med. Chem. Lett*. **2016**, *7*, 198-203.

(17) (a) Liu, Q.; Batt, D. G.; Lippy, J. S.; Surti, N.; Tebben, A. J.; Muckelbauer, J. K.; Chen, L.; An, Y.; Chang, C. Y.; Pokross, M.; Yang, Z.; Wang, H.; Burke, J. R.; Carter, P. H.; Tino, J. A. Design and synthesis of carbazole carboxamides as promising inhibitors of Bruton's tyrosine kinase (BTK) and Janus kinase 2 (JAK2). *Bio. Med. Chem. Lett.* **2015**, *25*, 4265-4269. (b) Liu, Q.; Batt, D. G.; De Lucca, G. V.; Shi, Q.; Tebben, A. J. U.S. Pat. Appl. Publ. US 20100160303 A1 20100624 (2010).

(18) Liu, L.; Halladay, J. S.; Shin, Y.; Wong, S.; Coraggio, M.; La, H.; Baumgardner, M.; Le, H.; Gopaul, S.; Boggs, J.; Kuebler, P.; Davis Jr., J. C.; Liao, X. C.; Lubach, J. W.; Deese, A.;

Sowell, C. G.; Currie, K. S.; Young, W. B.; Khojasteh, S. C.; Hop, C. E. C. A.; Wong, H. Significant species difference in amide hydrolysis of GDC-0834, a novel potent and selective Bruton's tyrosine kinase inhibitor. *Drug Met. Disp.* **2011**, *39*, 1840-1849.

(19) Plitnick, L. M.; Herzyk, D. J. The T-dependent antibody response to keyhole limpet hemocyanin in rodents. In; Dietert, R. R. (ed.). *Immunotoxicity testing: Methods and Protocols, Methods in Molecular Biology, Chapter 11.* **2009**, *598*, 159-171.

(20) Fabian, M. A.; Biggs III, W. H.; Treiber, D. K.; Atteridge, C. E.; Azimioara, M. D.; Benedetti, M. G.; Carter, T. A.; Ciceri, P.; Edeen, P. T.; Floyd, M.; Ford, J. M.; Galvin, M.; Gerlach, J. L.; Grotzfeld, R. M.; Herrgard, S.; Insko, D. E.; Insko, M. A.; Lai, A. G.; Lélias, J.-M.; Mehta, S. A.; Milanov, Z. V.; Velasco, A. M.; Wodicka, L. M.; Patel, H. K.; Zarrinkar, P. P.; Lockhart, D. J. A small molecule-kinase interaction map for clinical kinase inhibitors. *Nat. Biotechnol.* **2005**, *23*, 329-336.

(21) (a) Nandakumar, K. S.; Bäcklund, J.; Vestberg, M.; Holmdahl, R. Collagen type II (CII)-specific antibodies induce arthritis in the absence of T or B cells but the arthritis progression is enhanced by CII-reactive T cells. *Arthritis Res. Ther.* **2004**, *6*, R544-550. (b) Kagari, T.; Tanaka, D.; Doi, H.; Shimozato, T. Essential role of Fc gamma receptors in anti-type II collagen antibody-induced arthritis. *J. Immunol.* **2003**, *170*, 4318-4324.

(22) Street, L. J.; Baker, R.; Castro, J. L.; Chambers, M. S.; Guiblin, A. R.; Hobbs, S. C.; Matassa, V. G.; Reeve, A. J.; Beer, M.S. Synthesis and serotonergic activity of 5-(oxadiazolyl)tryptamines: potent agonists for 5-HT1D receptors. *J. Med. Chem.* **1993**, *36*, 1529–1538.

(23) Kamata, J.; Okada, T.; Kotake, Y.; Niijima, J.; Nakamura, K.; Uenaka, T.; Yamaguchi, A.; Tsukahara, K.; Nagasu, T.; Koyanagi, N.; Kitoh, K.; Yoshimatsu, K.; Yoshino, H.; Sugumi, H. A. Synthesis and evaluation of novel pyrimido-acridone, -phenoxadine, and -carbazole as topoisomerase II inhibitors. *Chem. Pharm. Bull Lett.* **2004**, *52*, 1071-1081.

(24) Shi, Q.; Tebben, A.; Dyckman, A. J.; Li, H.; Liu, C.; Lin, J.; Spergel, S.; Burke, J. R.; McIntyre, K. W.; Olini, G. C.; Strnad, J.; Surti, N.; Muckelbauer, J. K.; Chang, C.; An, Y.; Cheng, L.; Ruan, Q.; Leftheris, K.; Carter, P. H.; Tino, J.; De Lucca, G. V. Purine derivatives as potent Bruton's tyrosine kinase (BTK) inhibitors for autoimmune diseases. *Bio. Med. Chem. Lett.* **2014**, *24*, 2206-2211.

(25) (a) Zhang, J.; Shou, W. Z; Vath, M.; Kieltyka, K.; Maloney, J.; Elvebak, L.; Stewart, J.; Herbst, J.; Weller, H. N. An integrated bioanalytical platform for supporting high-throughput serum protein binding screening. *Rapid Commun. Mass Spec*., **2010**, *24*, 3593-3601 (protein binding). (b) Zvyaga, T. A.; Chang, S.-Y.; Chen, C.; Yang, Z.; Vuppugalla, R.; Hurley, J.; Thorndike, D.; Wagner, A.; Chimalakonda, A.; Rodrigues, A. D. Evaluation of six proton pump inhibitors as inhibitors of various human cytochromes P450: focus on cytochrome P450 2C19. *Drug Metab. Dispos*., **2012**, *40*, 1698-1711 (HLM CYP). (c) Cai, X.; Walker, A.; Cheng, C.; Paiva, A.; Li, Y.; Kolb, J.; Herbst, J.; Shou, W.; Weller, H. Approach to improve compound recovery in a high-throughput Caco-2 permeability assay supported by liquid chromatography–tandem mass spectrometry. *J. Pharm. Sci*., **2012**, *101*, 2755-2762 (Caco-2). (d) http://www.pion-inc.com/Products/PAMPA_Evolution/en (PAMPA). (e) Kieltyka, K.; Zhang, J.; Li, S.; Vath, M.; Baglieri, C.; Ferraro, C.; Zvyaga, T. A.; Drexler, D. M.; Weller, H. N.; Shou, W. Z. A high-throughput bioanalytical platform using automated infusion for tandem mass spectrometric method optimization and its application in a metabolic stability screen. *Rapid Commun. Mass Spec*., **2009**, *23*, 1579-1591 (liver microsome metabolic stability).

Figure 1. BTK Irreversible Inhibitors

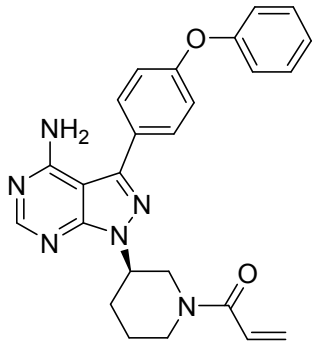

1, Ibrutinib

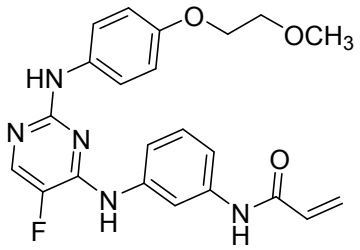

2

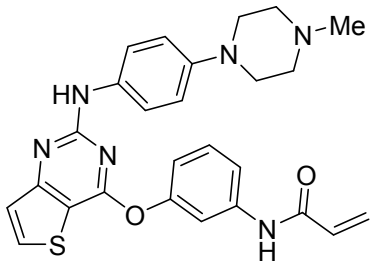

3

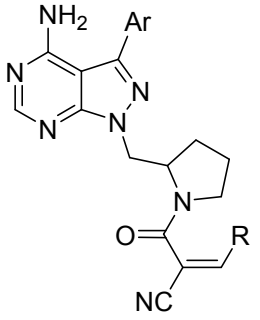

4a, generic Principia compound

Figure 2. Initial Lead 5 and Optimized Compound 6

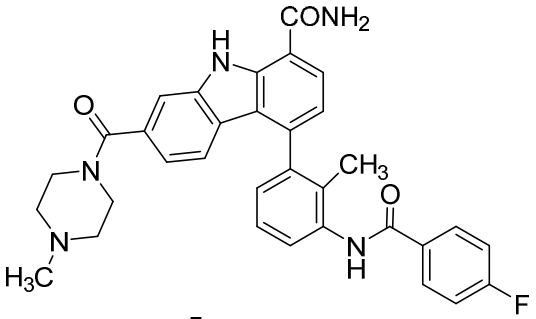

5

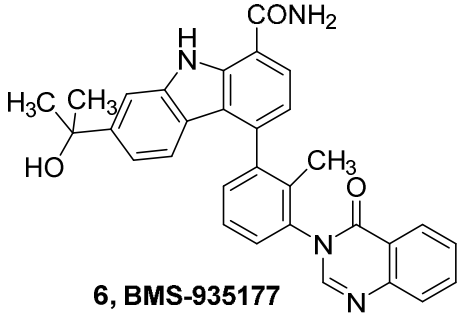

6, BMS-935177

Figure 3. Initial Optimization of Carbazole Core Series

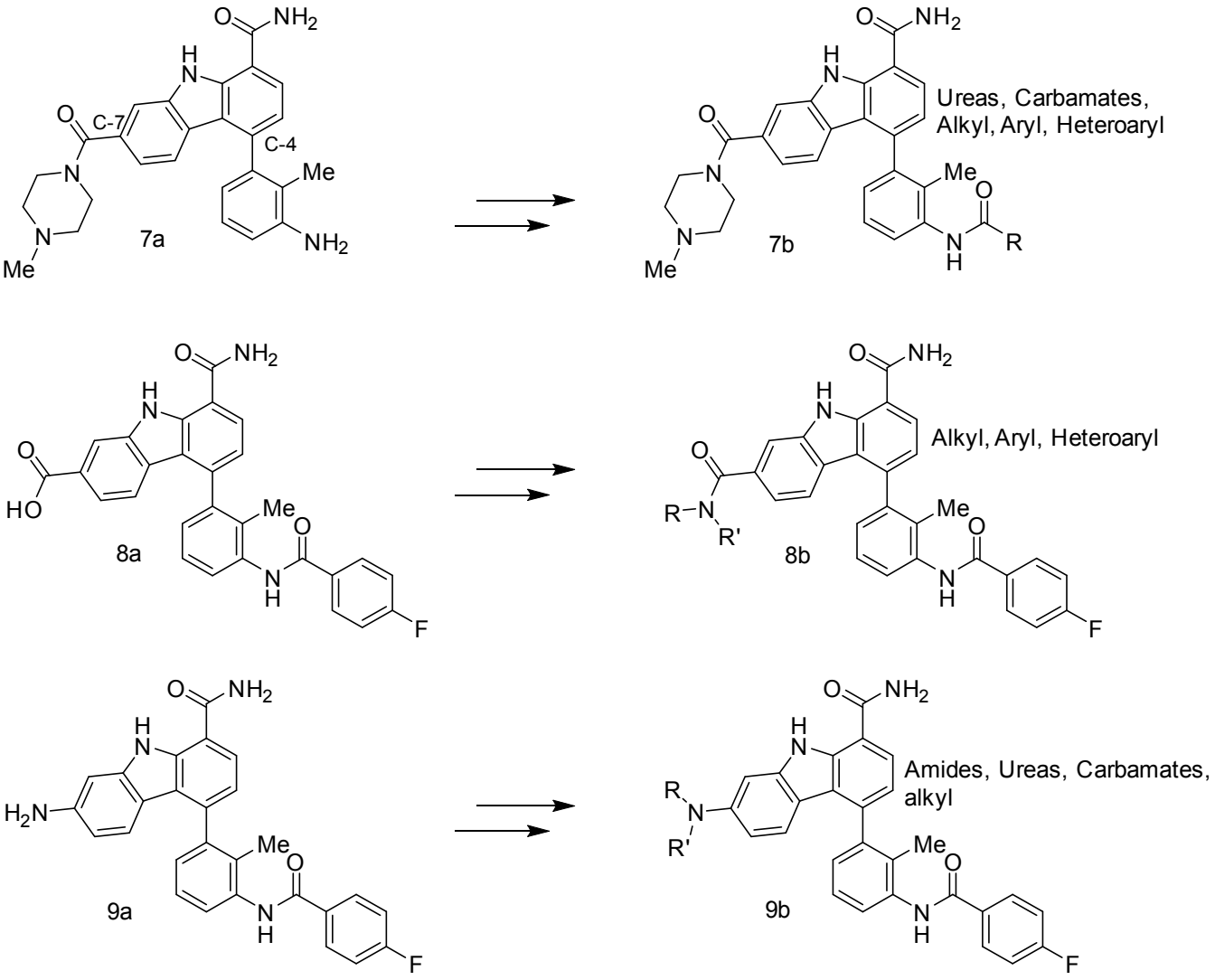

Figure 4 A, B. Compound 23 X-ray Crystal Structure Bound to BTK Kinase Domain[a]

A

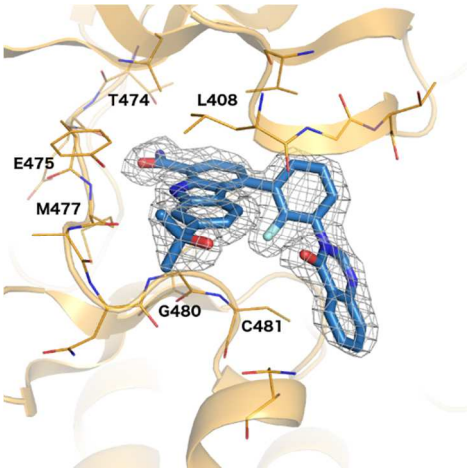

B

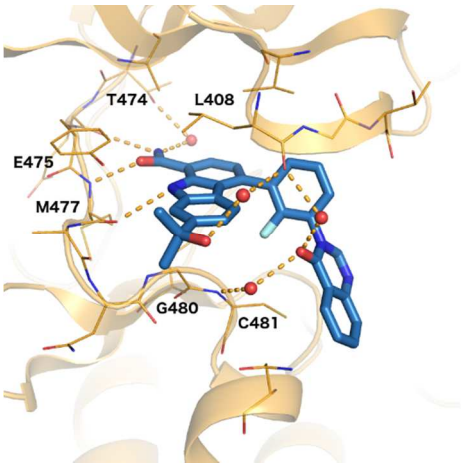

[a] 4a: electron density mapping of **23**; 4b, binding of **23 (PDB ID 5JRS)**, including waters.

Figure 5. A: Efficacy of 6 (5, 20, and 45 mg/kg) *vs.* Vehicle in a Mouse Neoantigen (KLH) Antibody Response Model. B: Plasma Exposures of 6 in Satellite Animals[a]

A

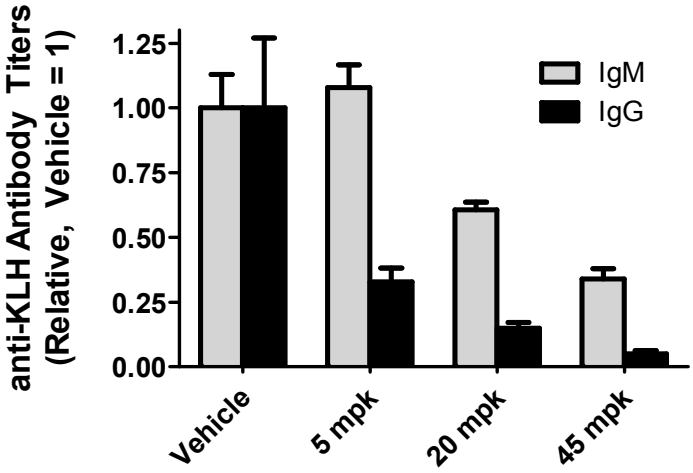

B

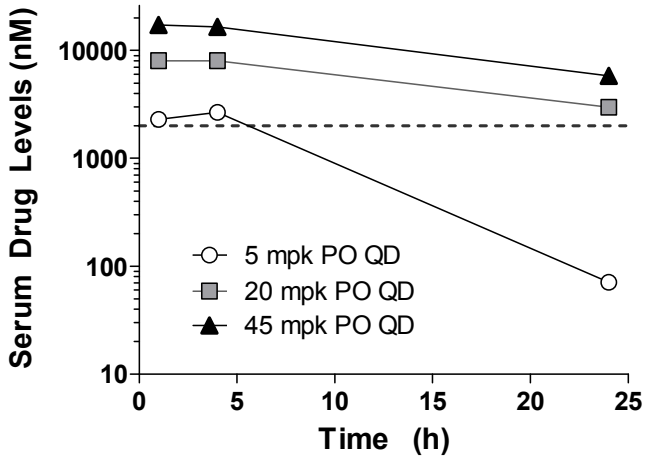

[a] Female BALB/c mice (8-12 weeks old, Harlan) were immunized IP with 250 µg KLH in PBS on Day 0. Mice were dosed daily by oral gavage with Vehicle (EtOH:TPGS:PEG300; 5:5:90) or Compound 6 at doses of 5, 20, or 45 mg/kg. Blood was collected on Days 7 and 14 post-immunization. Serum was separated and analyzed for anti-KLH IgM titers (Day 7) and anti-KLH IgG titers (Day 14) by ELISA. A, Day 7 IgM (gray bars) and day 14 IgG (dark bars) anti-KLH titers (*p<0.05 vs. vehicle, ANOVA with Dunnett's post-test); B, serum drug levels from day 1 satellite mice.

Figure 6. Efficacy of 6 (10, 20, and 30 mg/kg) *vs.* Vehicle in a Mouse Collagen Induced Arthritis (CIA) Inflammation Model[a]

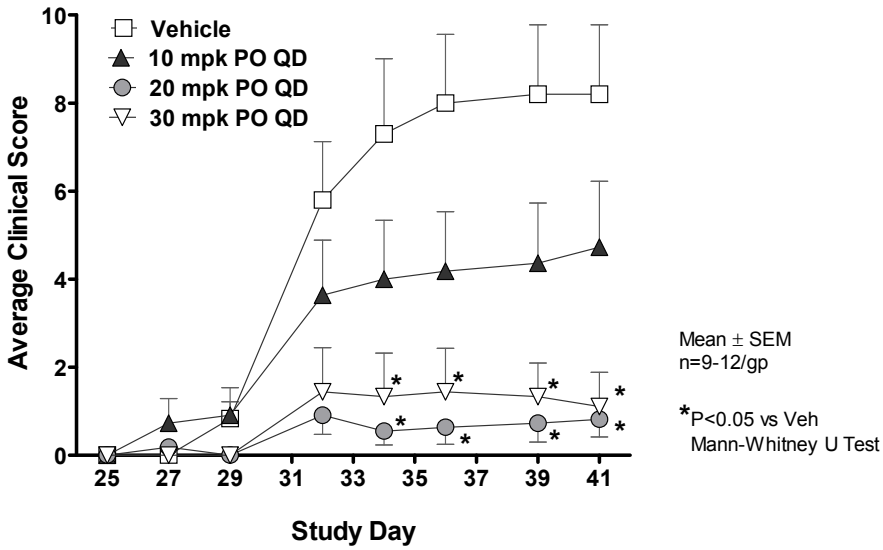

[a] DBA/1 male mice were immunized subcutaneously at the base of the tail on Day 0 and again on Day 21 with 200ug bovine type II collagen admixed with reconstituted Sigma Adjuvant System (SAS; Sigma-Aldrich). Mice were dosed daily by oral gavage with vehicle (EtOH:TPGS:PEG300; 5:5:90) or Compound 6 starting on day 0. Mice were monitored 3 times per week for the development and severity of paw inflammation. Clinical paw scores for all four paws were summed for each mouse, and mean ± SEM was calculated for each treatment group. *p value < 0.05 compared to vehicle treatment group.

Figure 7. Bone and Inflammation Efficacy of 6 (10, 20, and 30 mg/kg) *vs.* Vehicle in a Mouse CIA Model[a]

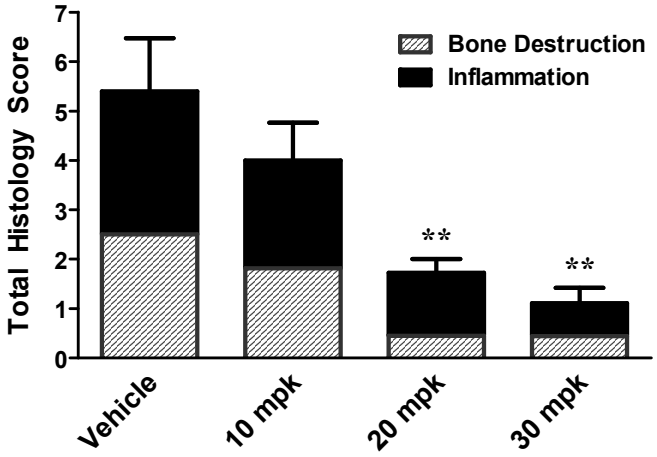

[a] Histological evaluation of rear paws from the CIA study. Lesions were scored on a severity scale of 0 (normal) to 4 in two separate categories, inflammation (cellular infiltration and pannus formation) and bone resorption. Results represent mean ± SEM. **p value < 0.01 compared to vehicle treatment group.

Figure 8. Representative µCT images of the hind paws of CIA mice treated with 6 (10, 20, and 30 mg/kg)[a]

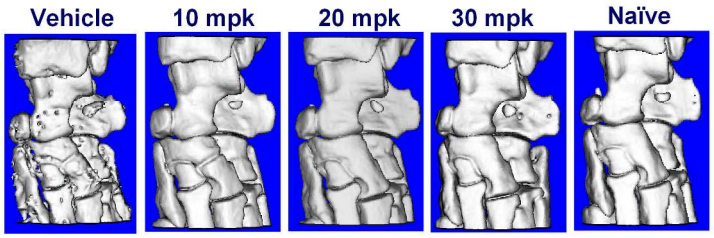

[a]Hind paws were excised postmortem and analyzed by micro-computed tomography (micro-CT) after fixation in 10% Neutral Buffered Formalin.

Figure 9. Efficacy of 6 (10 and 30 mg/kg) *vs.* Vehicle and Dexamethasone (Dex) in a Mouse Anti-Collagen Antibody-Induced Arthritis (CAIA) Inflammation Model[a]

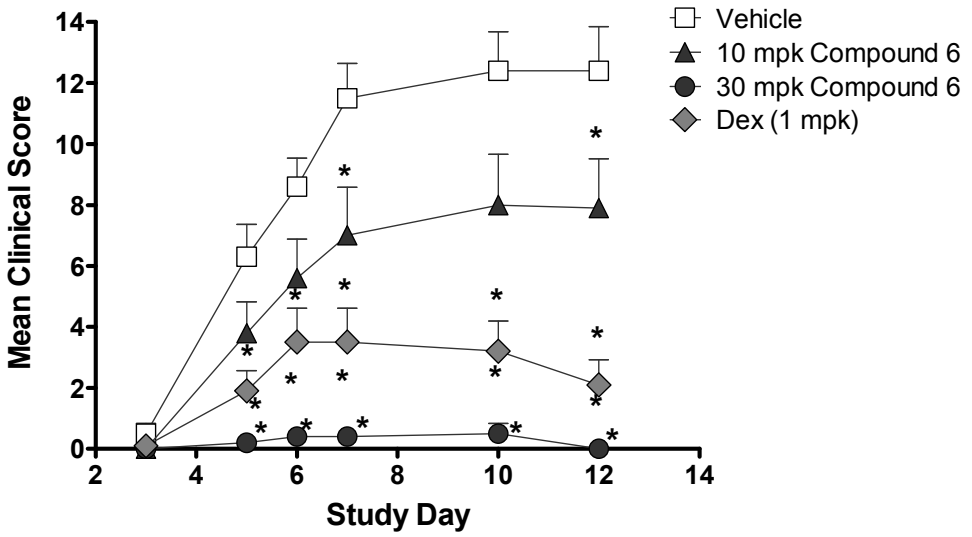

[a]Mice (N=8-10 per group) were injected intraperitoneally (IP) with a mixture of four monoclonal anti-mouse type II collagen antibodies (1 mg of each). Daily oral dosing was immediately started with Vehicle (EtOH:TPGS:PEG300; 5:5:90), Compound 6 (10 or 30 mg/kg) or dexamethasone (dex., 1 mg/kg). Three days later, the mice were injected IP with 1.25 mg/kg LPS (E. coli O111:B4; Sigma). Thereafter, mice were monitored 3X/wk for the development and severity of paw inflammation. Clinical scores are shown as mean ± SEM. * $p<0.05$ vs. vehicle group. n = 8-10/group.

Figure 10. A: Two Axes of Hindered Rotation of Compound 6. B: Chiral HPLC Trace Showing Four Atropisomers[a]

A

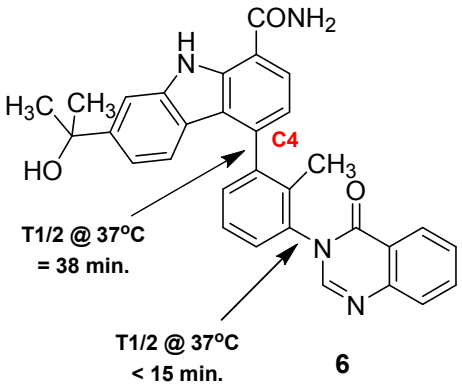

B

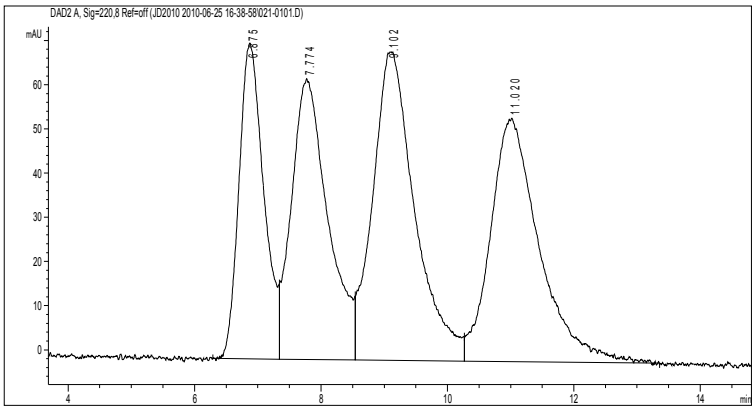

[a]A: Arrows showing bonds with hindered rotation leading to atropisomers. B: Chromatographic conditions: Chiralpak IB column, 4.6×250mm, 5µm, 35/65 MeOH/CO_2, 100 bar back pressure, 4mL/min, column 0°C.

Scheme 1. General Synthetic Route to Bicyclic Amide Replacements[a]

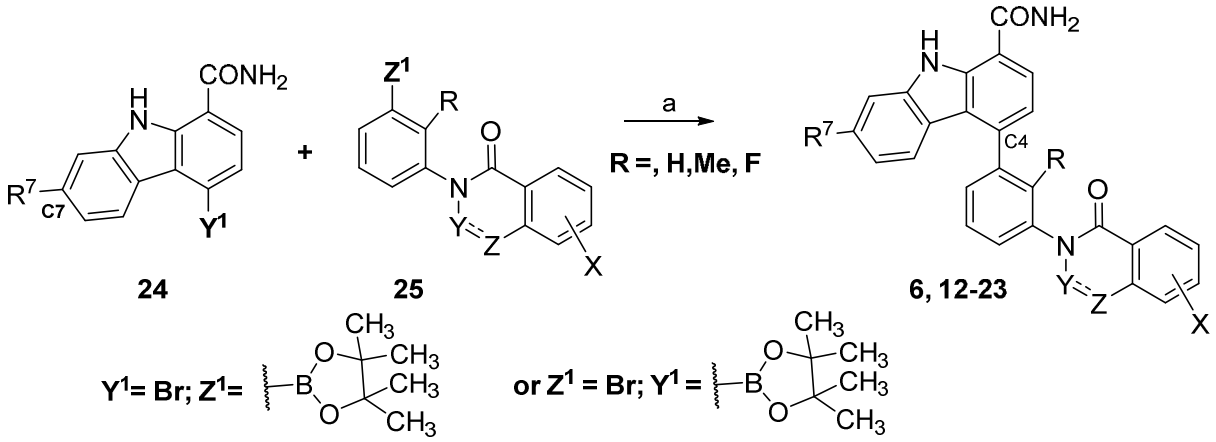

[a] Reagents and conditions: (a) Suzuki coupling conditions: $Pd(Ph_3P)_4$, 2 M K_3PO_4, toluene/ethanol (3/1), 100 °C, 16 h, 50-75%.

Scheme 2. Synthesis of Intermediates 31-33[a]

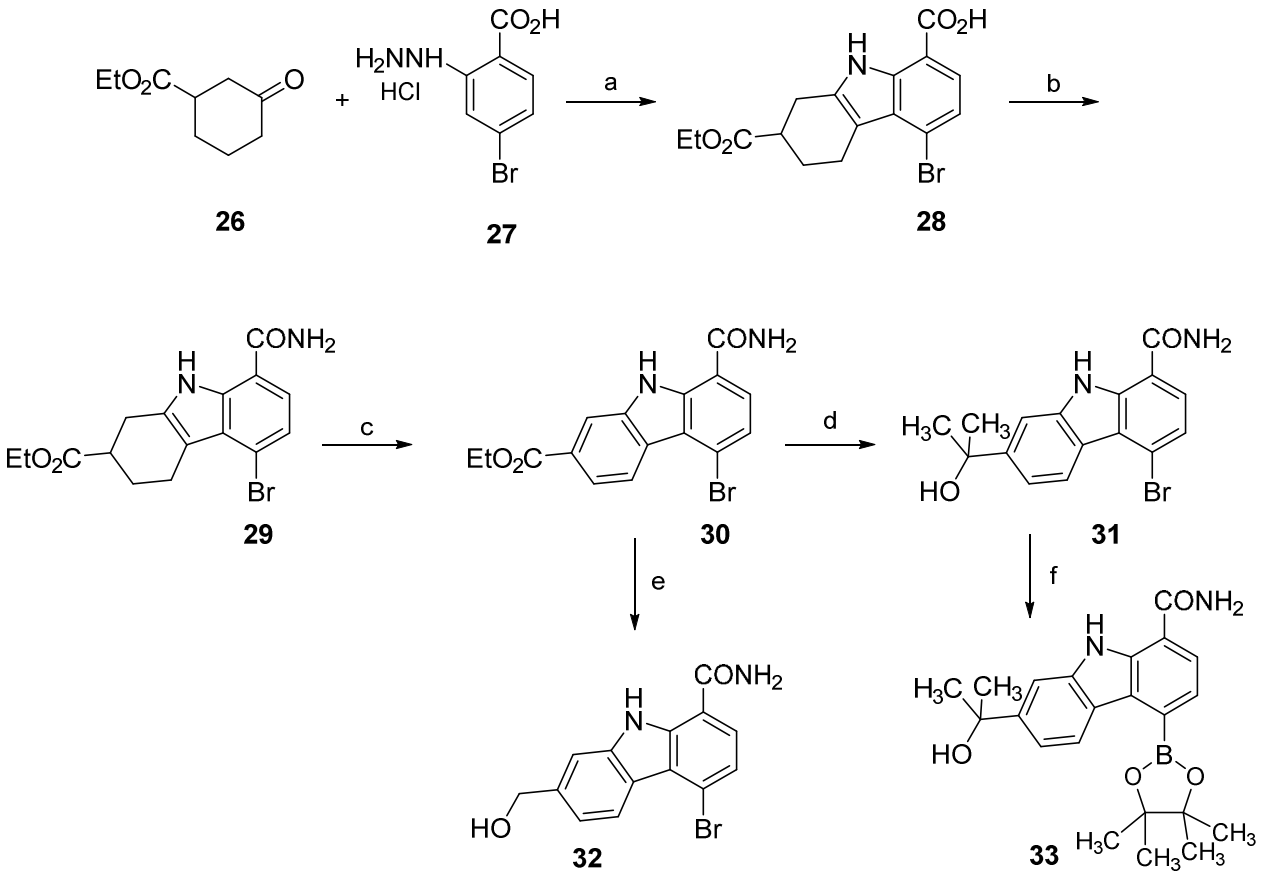

[a] Reagents and conditions: (a) AcOH, 110 °C, 3 h, 58%; (b) NH_4OH, EDC, HOBt, THF/DCM, rt, 16 h, 76%; (c) DDQ, THF, 0 °C to rt, 86%; (d) MeLi, -60 °C, THF, 84%; (e) LAH, THF, 0 °C, 64%; (f) 4,4,4',4',5,5,5',5'-octamethyl-2,2'-bis(1,3,2-dioxaborolane), $PdCl_2$dppf, KOAc, dioxane, 100 °C, 16 h, 70-85%.

Scheme 3. Synthesis of Intermediates 35 and 36[a]

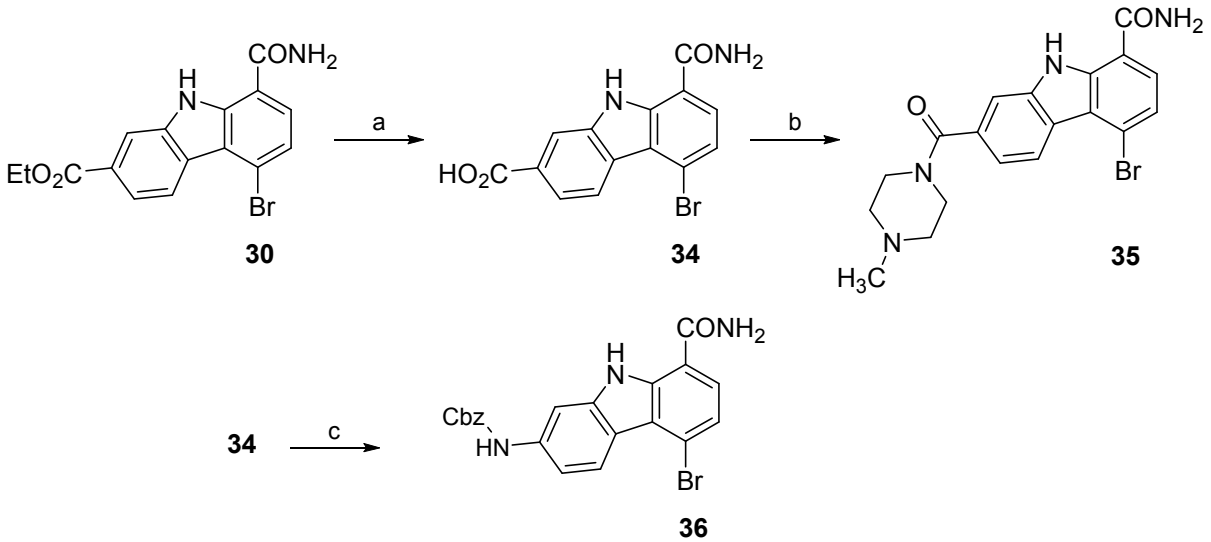

[a] Reagents and conditions: (a) LiOH, THF/ethanol/H_2O, reflux, 6 h, 96%; (b) 1-methylpiperazine, EDC, HOBt, THF/DCM, rt, 16 h, 96% (c) i) diphenylphosphoryl azide, Et_3N, dioxane, 50 °C, 1.5 h ii) benzylalcohol, 85 °C, 18 h, 91%.

Scheme 4. Synthesis of Compounds 5 and 11-12[a]

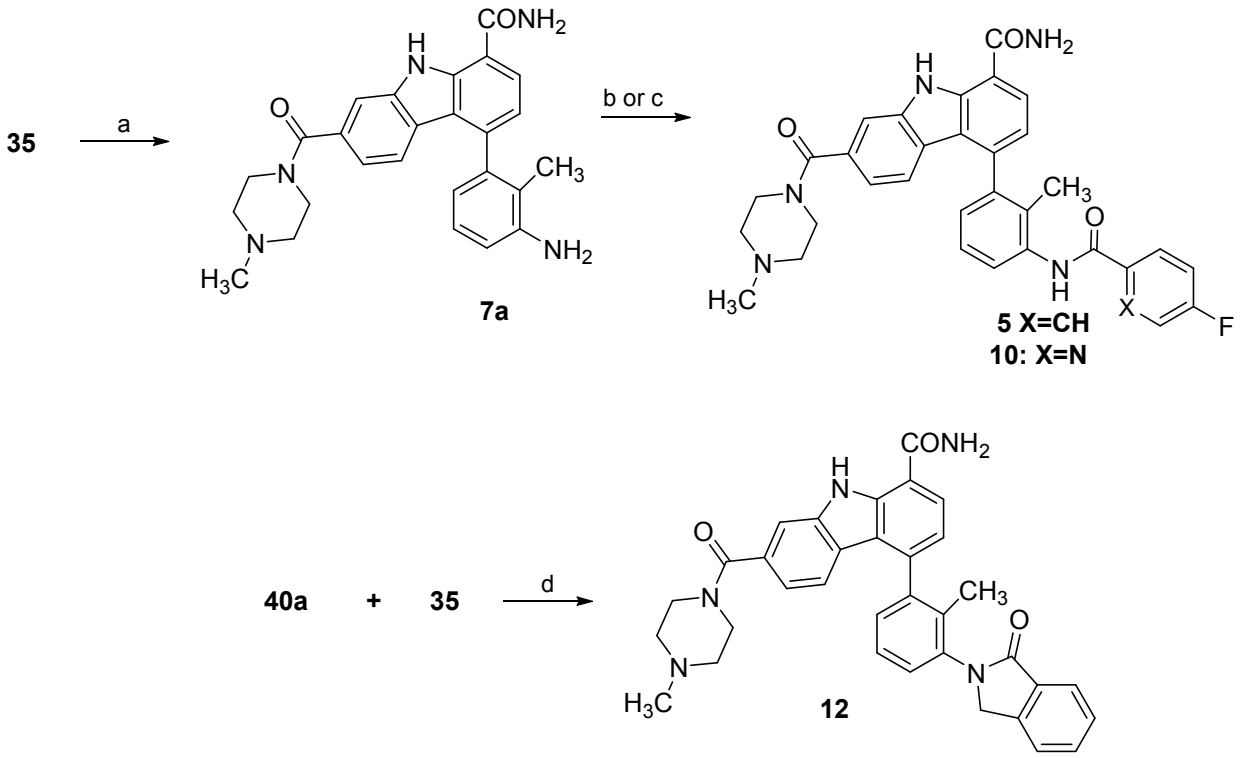

[a] Reagents and conditions: (a) 2-methyl-3-(4,4,5,5-tetramethyl-1,3,2-dioxaborolan-2-yl)aniline, $Pd(Ph_3P)_4$, 2 M K_3PO_4, toluene/ethanol(3/1), 100 °C, 16 h, 77%; (b) 4-F-benzoic acid, EDC, HOAt, DIEA, ACN, rt, 16 h, 92%; (c) 4-fluoropicolinic acid, EDC, HOAt, DIEA, ACN, rt, 18 h, 96%; (d) $Pd(Ph_3P)_4$, 2 M K_3PO_4, toluene/ethanol (3/1), 100 °C, 16 h, 60%.

Scheme 5. Synthesis of Boronic Ester Intermediates 40a and 40b[a]

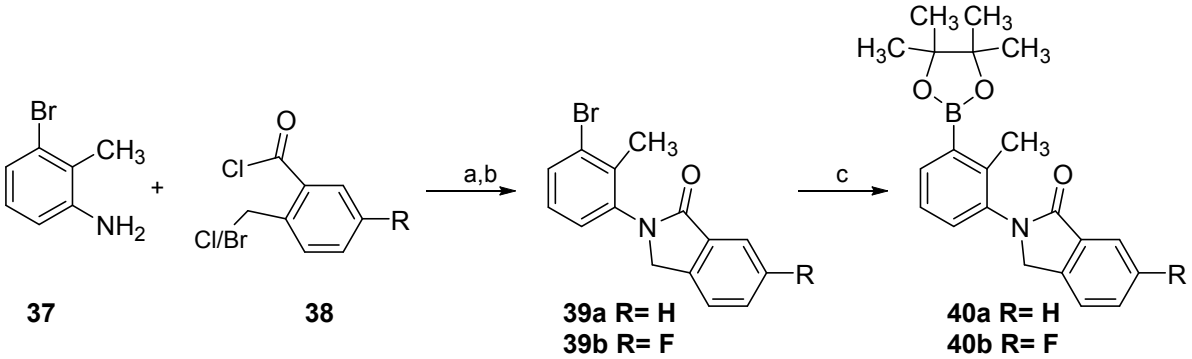

[a] Reagents and conditions: (a) Et_3N, DCM, rt, 2 h, 48%; (b) KOtBu, THF, rt, 1 h, 75%; (c) $PdCl_2dppf$, KOAc, dioxane, 100 °C, 16 h, 86%.

Scheme 6. Synthesis of Intermediates 44 and 47[a]

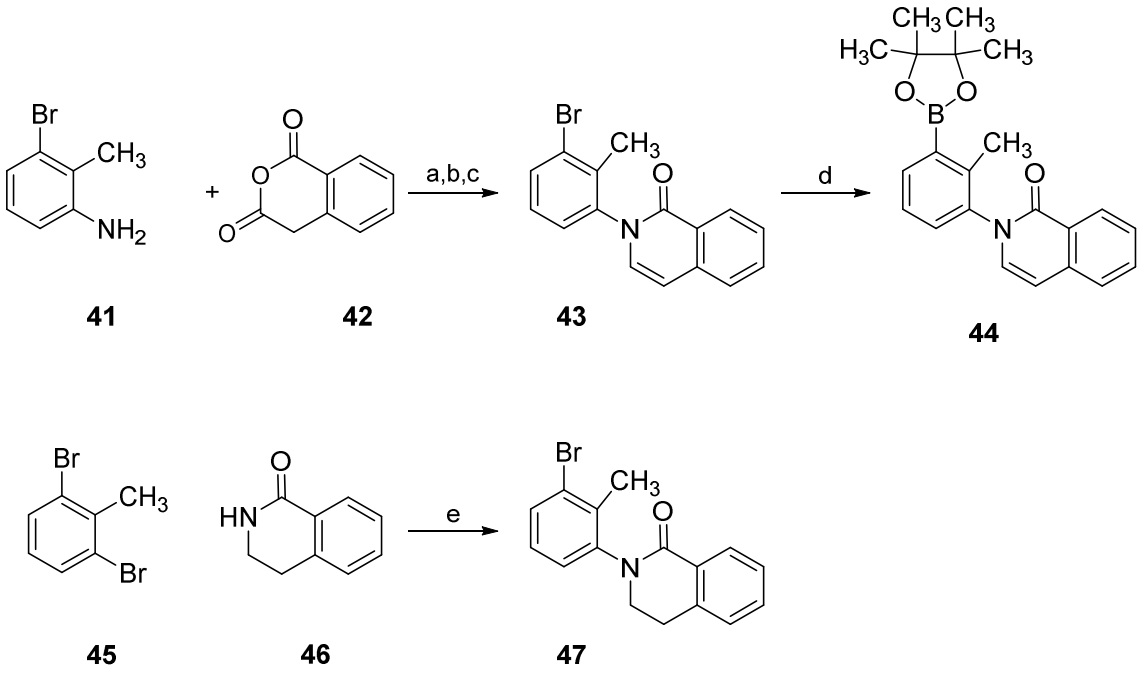

[a] Reagents and conditions: (a) AcOH, 110 °C, 16h, 36%; (b) $NaBH_4$, MeOH, rt, 6 h, 95%; (c) TFA, DCM, rt, 2 h, 67%; (d) $PdCl_2$dppf, KOAc, dioxane, 100 °C, 16 h, 67%. (e) CuI, K_2CO_3, DMSO, 150 °C, 1.5 h, 15%.

Scheme 7. Synthesis of Boronic Ester Intermediates 51[a]

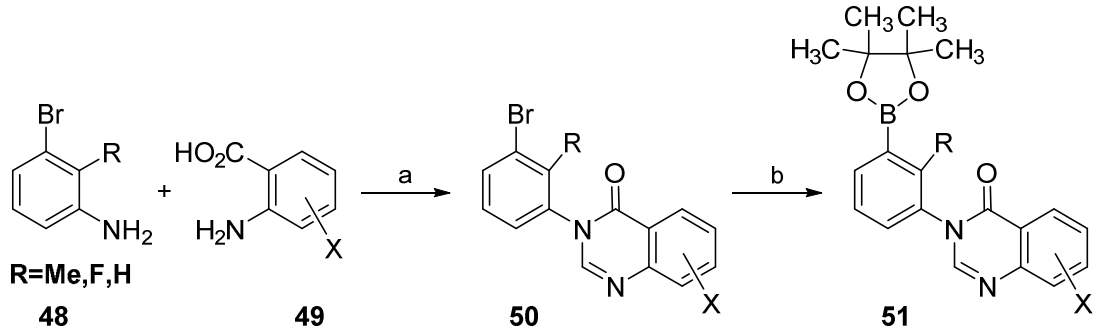

[a] Reagents and conditions: (a) Triethyl orthoformate, toluene, 110 °C, 16 h, 36-75%; (b) $PdCl_2$dppf, KOAc, dioxane, 100 °C, 16 h, 67- 95%.

Table 1. *In Vitro* Potency, Selectivity and Mouse PK of Carbazole Analogues

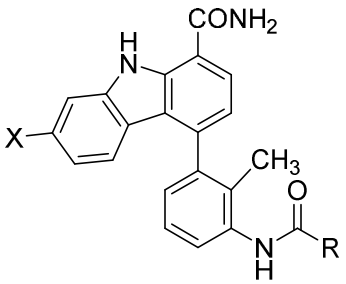

Cmpd	X	R	BTK[a] IC_{50} (nM)	LCK/ BTK[b]	PAMPA[c] Pc (nm/s)	CMax[d] (nM)	AUC[e] (uM*hr)
5	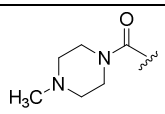	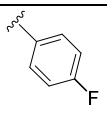	5 ±2	15x	147	90	0.4

10	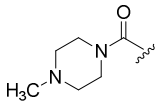	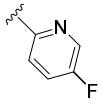	9 ±8	9x	587	1570	5
11	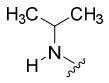	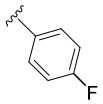	11 ±2	61x	Null[f]	7960	36

[a]IC_{50} values are shown as mean values of three determinations. [b]Fold enzyme IC_{50} selectivity. [c] PAMPA values were determined at pH 7. [d,e]CMAX (maximum concentration) and AUC0-24 hr (area under the curve), respectively, after 10 mg/kg oral dosing in male Balb/C mice with PEG300/TPGS/ethanol (90/5/5 v/v/v) vehicle. [f] Null = compound was not detected.

Table 2. ***In Vitro*** **Potency, Selectivity and Mouse PK of Carbazole Analogues**

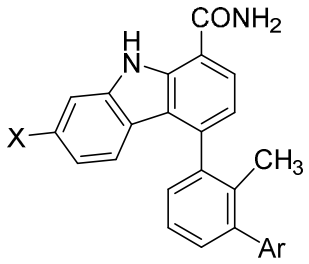

Cmpd	X	Ar	BTK[a] IC_{50} (nM)	LCK/ BTK[b]	Ramos[a] IC_{50} (nM)	CMax[c] (nM)	AUC[d] (uM*hr)
12	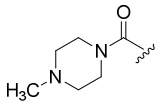	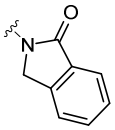	5 (n=2)	14x	238 ±90	178	0.3
13		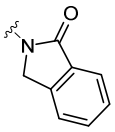	5 (n=2)	25x	154[e]	ND[f]	ND[f]
14		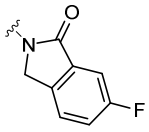	2 ±1	48x	48 ±30	4410	41
15		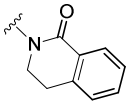	3[e]	33x	26[e]	ND[f]	ND[f]
16		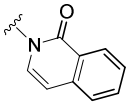	5[e]	44x	144[e]	ND[f]	ND[f]
6		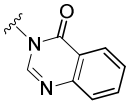	3 ±1	56x	26 ±15	8960	80

17		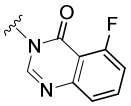	5[e]	61x	18 (n=2)	6740	58
18		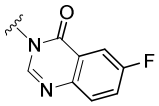	7[e]	52x	40 ±20	9770	113
19		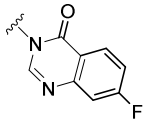	2 (n=2)	89x	24 (n=2)	8060	120
20		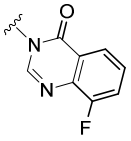	2 ±1	88x	34 ±25	6850	63
21		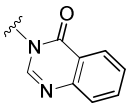	3[e]	146x	22 (n=2)	4650	14

[a]IC_{50} values are shown as mean values of at least three determinations. [b]Fold enzyme IC_{50} selectivity. [c,e]CMAX (maximum concentration) and AUC0-24 hr (area under the curve), respectively, after 10 mg/kg oral dosing in male Balb/C mice with PEG300/TPGS/ethanol (90/5/5 v/v/v) vehicle. [e]IC_{50} values are shown as single determinations. [f]ND = Not Determined.

Table 3. *In Vitro* Potency, Selectivity and Mouse PK of Carbazole Analogues

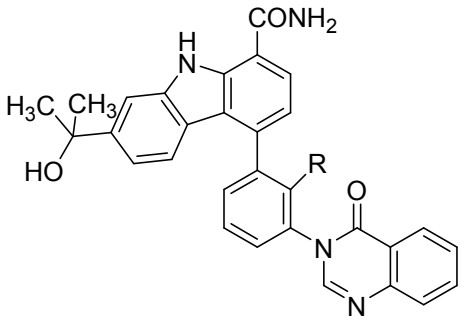

Cmpd	R	BTK[a] IC_{50} (nM)	LCK/ BTK[b]	Ramos[a] IC_{50} (nM)	CMax[c] (nM)	AUC[d] (uM*hr)
22	**H**	44[e]	32x	410[e]	ND[f]	ND[f]
23	**F**	4 ±2	210x	30 ±2	2100	19

[a]IC_{50} values are shown as mean values of at least three determinations. [b]Fold enzyme IC_{50} selectivity. [c,e]CMAX (maximum concentration) and AUC0-24 hr (area under the curve), respectively, after 10 mg/kg oral dosing in male Balb/C mice with PEG300/TPGS/ethanol (90/5/5 v/v/v) vehicle. [e]IC_{50} values are shown as single determinations. [f]ND = Not Determined.

Table 4. Partial List of *In Vitro* Kinase Selectivity Data for Compound 6

Kinase	IC_{50}, μM	Fold BTK Selectivity
TEC	0.013	5
BMX	0.024	9
ITK	0.096	28
TXK	0.180	67
BLK	0.020	7
TRKA	0.030	11
HER4	0.050	18
TRKB	0.10	35
RET	0.11	40
LCK	0.15	55
LYN	0.16	60
SRC	3.19	1140
JAK2	0.37	131

Table 5. Partial List of *In Vitro* Cell Activity Data for Compound 6[a]

cellular assay	receptor/ stimulation	IC_{50}, μM
Calcium Flux in Ramos B Cells	BCR/Anti-IgM	0.026 ±0.015
Proliferation of human tonsillar B Cells	BCR/Anti-IgM/IgG	0.008[b]
CD69 surface expression in peripheral B Cells	BCR/Anti-IgM/IgG	0.008[b]
CD69 surface expression in peripheral B Cells	CD40/CD40L	>10
TNFα from human PBMC Cells	FCλR/ Immune Complex	0.014[b]
Human whole blood CD69 surface expression in peripheral B Cells	BCR/Anti-IgM	0.55 ±0.1
Mouse whole blood CD69 surface expression in peripheral B Cells	BCR/Anti-IgM/IgG	2.06 ±0.24

[a]IC_{50} values are shown as mean + standard deviation values of at least three determinations. [b]IC_{50} values are shown as single determinations.

Table 6. Partial List of *In Vitro* Profiling Data for Compound **6**[a]

parameter	result
protein binding[a]	99.4% in human serum
	99% in mouse serum
mutagenicity	Ames negative
hERG (patch clamp)	55% inhibition @ 10 μM
CYP[b] inhibition (IC_{50})[a]	>40 μM 1A2, 2B6, 2D6, 3A4; >8 μM 2C9, 2C8
aqueous solubility	< 1 μg/mL
FaSSIF solubility[c]	6 μg/mL
FeSSIF solubility[d]	60 μg/mL
PAMPA (pH 5.5/7.4)[a]	876 and 1023 nm/s
Caco2 Permeability[a] (apical to basolateral)	<15 nm/s

(basolateral to apical)	122 nm/s

[a]See reference 25 for assay methods. [b]CYP = cytochrome P450; HLM CYP assay. [c]FaSSIF = Fasted State Simulated Intestinal Fluid. [d]FeSSIF = Fed State Simulated Intestinal Fluid.

Table 7. Pharmacokinetic Parameters for Compound 6[a]

parameter	mouse	rat[a]	dog[a]	cyno[a]
po dose (mg/kg)	5[b]	5[b]	2[b]	2[b]
iv dose (mg/kg)	2	2	2	2
C_{max} (μM), PO	3.8	2.0	1.2 ± 0.3	4.8 ± 0.6
T_{max} (μM), PO	3.0	5.0	1.6 ± 0.7	2.7 ± 1.2
AUC (μM*h), PO	30.8	21.2	14.2 ± 2.1	32 ± 7.2
$T_{1/2}$ (h), iv	4.0	5.1 ± 0.1	10.4 ± 2.1	10.6 ± 1.2
Cl (mL/min/kg), iv	4.9	6.4 ± 0.9	3.7 ± 0.3	2.1 ± 0.6
V_{ss} (L/kg), iv	1.7	2.6 ± 0.2	3.2 ± 1.0	1.6 ± 0.2
F_{po} (%)	94	84	100 ± 8	100

[a]Average of three animals with associated standard deviation. [b]Vehicle: PEG400/water/ethanol (70/20/10 v/v/v).

Table of Contents Graphic

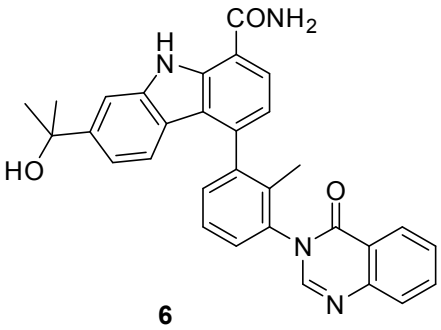

6